Peer-reviewed version available at *Processes* **2020**, *8*, 1006; doi:10.3390/pr8081006

Type of the Paper (Review)

Optimization of magnetic properties of magnetic microwires by Post-processing.

Valentina Zhukova[1,2], Paula Corte-Leon[1,2], Lorena González-Legarreta[1,3], Ahmed Talaat[1,4], Juan Maria Blanco[2], Mihail Ipatov[1], Jesus Olivera[5,6] and Arcady Zhukov[1,2,7]*,

Keywords

[1] Dept. Mater. Phys., Faculty of Chemistry, University of Basque Country, UPV/EHU, 20018 San Sebastian, Spain; paula.corte@ehu.eus (P.C.-L.); valentina.zhukova@ehu.es (V.Z.); mihail.ipatov@ehu.es (M.I.)
[2] Department Applied Physics I, EIG, University of Basque Country, UPV/EHU, 20018, San Sebastian, Spain; juanmaria.blanco@ehu.es (J.M.B.)
[3] Dept. QUIPRE, Inorganic Chemistry-University of Cantabria, Nanomedice-IDIVAL, Avda. de Los Castros 46, 39005 Santander, Spain, lorena.glegarreta@gmail.com (L.G.L)
[4] Department of Mechanical Engineering & Materials Science, Swanson School of Engineering, University of Pittsburgh, Pittsburgh, PA, 15261, USA, aht17@pitt.edu (A.T.)
[5] Pontificia Universidad Católica Madre y Maestra, Santo Domingo, P.O. Box 2748, Dominican Republic; jesus.oliveradga@gmail.com (J.O.)
[6] Laboratorio de la Dirección General de Aduanas, Santo Domingo, Dominican Republic, jesus.oliveradga@gmail.com (J.O.)
[7] IKERBASQUE, Basque Foundation for Science, 48011 Bilbao, Spain; arkadi.joukov@ehu.es (A.Z.)
* Correspondence arkadi.joukov@ehu.es; Tel.: +34-943-01-8611 (A.Z.)

Abstract: The influence of post-processing conditions on the magnetic properties of amorphous and nanocrystalline microwires have been thoroughly analyzed, paying attention on the influence of magnetoelastic, induced and magnetocrystalline anisotropies on the hysteresis loops of Fe-, Ni- and Co-rich microwires. We showed that magnetic properties of glass-coated microwires can be tuned by the selection of appropriate chemical composition and geometry in as-prepared state or further considerably modified by appropriate post-processing, which consists of either annealing or glass-coated removal. Furthermore, stress-annealing or Joule heating can further effectively modify the magnetic properties of amorphous magnetic microwires owing to induced magnetic anisotropy. Devitrification of microwires can be useful for either magnetic softening or magnetic hardening of the microwires. Depending on the chemical composition of the metallic nucleus and on structural features (grain size, precipitating phases) nanocrystalline microwires can exhibit either soft magnetic properties or semi-hard magnetic properties. We demonstrated that the microwires with coercivities from 1 A/m to 40 kA/m can be prepared.

Keywords: Magnetic microwires; post-processing; hysteresis loops; magnetic anisotropy;

1. Introduction

Development of magnetic sensors is essentially influenced by the technological progress in the field of magnetic materials [1-3]. Indeed, the features of magnetic sensors are determined by selection of appropriate magnetic material. A significant portion of magnetic sensors use soft magnetic materials [3].

One of the most promising families of soft magnetic materials with a number of advantages, such as excellent magnetic softness, fast and inexpensive manufacturing process, dimensionality suitable for various sensor applications, and good mechanical properties, is a family of amorphous and nanocrystalline materials obtained using rapid quenching from the melt [4-6].

Peer-reviewed version available at Processes 2020, 8, 1006; doi:10.3390/pr8081006

Such advanced functional magnetic properties have been reported in amorphous materials with either planar (ribbons) or cylindrical (wires) geometry [4-6]. However, each family of amorphous materials presents specific features making them suitable for rather different applications. Thus, planar (ribbon-shaped) materials with low magnetic losses and high saturation magnetization values are good for applications in transformers [4]. On the other hand, amorphous wires can present quite peculiar magnetic properties, such as spontaneous magnetic bistability associated with single and large Barkhausen jump [7-9] or giant magnetoimpedance, GMI, effect [10-13]. Although it is worth mentioning that in fact, large Barkhausen and GMI effect can be observed either in crystalline wires [14,15] as well as in properly heat treated amorphous ribbons [16,17]. However, high GMI effect and extremely fast single domain wall, DW, propagation can be realized in amorphous magnetic wires in a most simple way (i.e., even without additional post-processing) [18-20].

These features can be attributed to the fact that the cylindrical geometry together with the internal stresses distribution typical for the rapid quenching from the melt provide the unique features, like core-shell domain structure presenting either high circumferential magnetic permeability (in negative magnetostrictive Co-rich compositions) or existence of axially magnetized single inner domain responsible for observation of the single and large Barkhausen jump and related single DW propagation [19,20]. The cylindrical geometry in fact is suitable for realization of the aforementioned unique magnetic properties not only in magnetic wires prepared involving rapid melt quenching, but even in conventional magnetic wires [14,15] and even in nanowires prepared using i.e., electrodeposition [21,22].

It is worth mentioning that recent progress in rapidly quenched technology allows considerable dimensionality reduction of rapidly quenched materials [20,23,24]. Therefore, features reported in rapidly quenched amorphous materials can be useful for nanotechnology.

As mentioned above, most of the studies are related (although not limited) to either GMI effect or single DW dynamics. As regarding the GMI effect, the main interest is related to extremely high impedance sensitivity to an external magnetic field (up to 10 %/A/m) observed in properly prepared and processed magnetic microwires [10-13,18,25,26]. Such features of the GMI effect observed in amorphous wires allowed the development of the GMI technology suitable for numerous applications, such as magnetic compass and acceleration sensors integrated in complementary metal-oxide-semiconductor (CMOS) circuits [27,28], reduced-sized magnetometer suitable for magnetic field mapping [29,30], detection of a biomagnetic field with the pico-Tesla sensitivity [31], magnetoelastic and temperature sensors [32,33].

A variety of technological applications require miniaturization combined with excellent corrosion and mechanical properties and biocompatibility of the magnetic elements [2-4, 12-14]. This combination of physical properties and reduced dimensions can be achieved in glass-coated microwires: among the rapid melt quenching methods, the so-called Taylor-Ulitovsky method allows preparation of the thinnest amorphous wires covered by flexible and insulating glass [34-37]. It is worth mentioning that the method itself is known since the 60-s [34] and the preparation of magnetic amorphous microwires has been reported since the 70-s [18,35,36]. The preparation method consists in the fabrication of glass-coated microwires with metallic nucleus, diameters typically from submicrometric up to 40 μm, by simultaneous rapid melt quenching of metallic alloy covered by insulating glass coating [36]. This method is suitable for fabrication of magnetic microwires with either amorphous or nano-micro crystalline structure [18,23-25,33,36-38].

A variety of magnetic properties interesting for various technological applications, such as high GMI effect (up to 650% GMI ratio) [18,25,26], extremely fast single domain wall (DW) propagation (with DW velocity up to 3 km/s) [19,23,24,38], considerable magnetoresistance [36,39] and magnetocaloric [36,40] effects or even semi-hard magnetic properties [36,41] have been reported for glass-coated microwires.

As discussed elsewhere [36], the magnetic properties of microwires to a great extent are determined by the microstructure of the metal core. The microstructure depends on fabrication conditions, like the quenching rate as well as the chemical composition of the metallic nucleus alloy.

Preprints (www.preprints.org) | NOT PEER-REVIEWED | Posted: 7 July 2020 doi:10.20944/preprints202007.0107.v1

Peer-reviewed version available at Processes 2020, 8, 1006; doi:10.3390/pr8081006

Thus, if the quenching rate achieved during the quenching process from the melt is not high enough, metastable crystalline microwires with crystalline structure of metallic alloy nucleus can be prepared [36,40,41]. However, even magnetic properties of amorphous microwires are affected by the fabrication conditions (like quenching rate or glass-coating thickness) and chemical composition of the metallic alloy [18,43,44]. This compositional dependence is related to the magnetoelastic anisotropy affected by the magnetostriction coefficient as well as by the internal stresses values [18,43-47]. However, appropriate post- processing is the other factor allowing either fine tuning or even drastic modification of magnetic properties [43,44,48].

In this review, we have analyzed the influence of various factors on the magnetic properties of glass-coated microwires and provide the guideline for selection of appropriate post-processing for optimization of properties of magnetic microwires.

2. Experimental Methods and Materials

We prepared and analyzed amorphous glass-coated microwires based on Fe-, Co- and Ni- alloys with minor metalloid additions (Si, B, C) necessary for preparation of amorphous alloys [6-8, 12, 36]. Employed Taylor-Ulitovsky technique is earlier described elsewhere [36].

Table 1. Compositions and geometry of studied glass-coated microwires.

Composition	Metallic nucleus diameter, d (μm)	Total diameter, D (μm)	Ratio ρ=d/D	Magnetostriction coefficient, λ_s x10^{-6}
$Fe_{75}B_9Si_{12}C_4$	15.2	17.2	0.88	38
$Fe_{62}Ni_{15.5}Si_{7.5}B_{15}$	14.35	33.25	0.43	27
$Fe_{49.6}Ni_{27.9}Si_{7.5}B_{15}$	14.2	33.85	0.42	20
$Co_{70.5}Mn_{4.5}Si_{10}B_{15}$	10	26	0.38	-0.2
$Co_{77.5}Si_{15}B_{7.5}$	13.1	18	0.73	-5
$Co_{69.2}$ $Fe_{3.6}Ni_1B_{12.5}Si_{11}$ $C_{1.2}Mo_{1.5}$	22.8	23.2	0.98	-1
$Co_{68.5}Si_{14.5}B_{14.5}Y_{2.5}$	5	22	0.23	-5
$Co_{65.4}Fe_{3.8}Ni_1B_{13.8}Si_{13}C_{1.65}Mo_{1.35}$	18.8	22.2	0.85	-1
$Co_{67}Fe_{3.85}Ni_{1.45}B_{11.5}Si_{14.5}Mo_{1.7}$	6.6	15.7	0.42	-3
$Co_{67}Fe_{3.85}Ni_{1.45}B_{11.5}Si_{14.5}Mo_{1.7}$	6.8	13.6	0.5	-3
$Co_{67}Fe_{3.85}Ni_{1.45}B_{11.5}Si_{14.5}Mo_{1.7}$	9.8	18.5	0.53	-3
$Co_{67}Fe_{3.85}Ni_{1.45}B_{11.5}Si_{14.5}Mo_{1.7}$	11.8	18.4	0.64	-3
$Co_{67}Fe_{3.85}Ni_{1.45}B_{11.5}Si_{14.5}Mo_{1.7}$	13.4	20.9	0.64	-3
$Co_{67}Fe_{3.85}Ni_{1.45}B_{11.5}Si_{14.5}Mo_{1.7}$	16.8	24	0.7	-3
$Co_{67}Fe_{3.85}Ni_{1.45}B_{11.5}Si_{14.5}Mo_{1.7}$	16.8	21	0.8	-3
$Co_{69.2}Fe_{4.1}B_{11.8}Si_{13.8}C_{1.1}$	25.6	30.2	0.85	-0.03
$Fe_{71,8}Cu_1Nb_{3,1}Si_{15}B_{9,1}$	7.0	24.8	0.282	30
$Fe_{71,8}Cu_1Nb_{3,1}Si_{15}B_{9,1}$	18.2	39	0.467	30
$Fe_{70.8}Cu_1Nb_{3.1}Si_{14.5}B_{10.6}$	11.8	14.4	0.8	30
$Co_{67}Fe_{3.9}Ni_{1.5}B_{11.5}Si_{14.5}Mo_{1.6}$	25.6	26.6	0.96	-0.29
$Co_{68.7}Fe_4Ni_1B_{13}Si_{11}Mo_{2.3}$	17	23.6	0.72	-1.06
$Fe_{38.5}Co_{38.5}B_{18}Mo_4Cu_1$	9.4	22.5	0.41	
$Fe_{38.5}Co_{38.5}B_{18}Mo_4Cu_1$	10	16.6	0.6	
$Fe_{50}Pt_{40}Si_{10}$	8	21	0.38	

The structure of the samples has been analyzed by the X-ray Diffraction (XRD) as well as by the Differential Scanning Calorimeter (DSC). The BRUKER (D8 Advance) X-ray diffractometer with Cu K_α (λ =1.54 Å) radiation has been used in the XRD studies. All amorphous (as-prepared or annealed)

Preprints (www.preprints.org) | NOT PEER-REVIEWED | Posted: 7 July 2020 doi:10.20944/preprints202007.0107.v1

Peer-reviewed version available at Processes 2020, 8, 1006; doi:10.3390/pr8081006

microwires present a broad halo typical for completely amorphous materials. The DSC studies were performed using a 204 F1 Netzsch calorimeter.

The microwires were annealed at a temperature, T_{ann}, in the range from 200 °C to 400 °C in a conventional furnace in order to avoid the crystallization typically reported for $T_{ann} \geq 490$ °C [49]. The advantage of amorphous microwires is their superior mechanical properties typically reported for amorphous materials [50,51]. Typically, we fixed annealing time, t_{ann}, of 60 min as commonly used for heat treatment of amorphous and nanocrystalline materials [48,49].

In the case of stress-annealing, the tensile stress was applied during the annealing, as well as during the sample cooling in the furnace. The stress value in the metallic nucleus, σ_m, was evaluated considering different Young's modulus of metal, E_2, and glass, E_1, as following [43,48,52]:

$$\sigma_m = \frac{K \cdot P}{K \cdot S_m + S_{gl}} \qquad (1)$$

where $K=E_2/E_1$, P is the applied mechanical load and S_m, and S_{gl} are the cross sections of the metallic nucleus and the glass coating, respectively.

Hysteresis loops have been recorded using the fluxmetric method adapted for studies of magnetic microwires [49]. Hysteresis loops can be represented as the normalized magnetization, M/M_o, versus the applied magnetic field, H, where M_o is the magnetic moment of the sample at the maximum magnetic field amplitude, H_o [49,53].

The magnetostriction coefficient, λ_s, of the studied microwire, was evaluated by the SAMR method recently adapted for microwire [54,55]. In this method λ_s -values are determined in the microwire saturated by an axial magnetic field, H. Simultaneously, low AC transverse field, H_c, generated by an AC electric current flowing along the microwire allows a reversible magnetization rotation. More detailed SAMR method description and of the set-up adapted for evaluation of magnetostriction coefficient in microwires are provided elsewhere [54,55].

The glass coating was removed from the microwires by chemical etching using diluted (10%) hydrofluoric (HF) acid.

3. Results and Discussion

Below we have summarized the highlight findings already published and also the obtained recently experimental results on tailoring of magnetic properties of glass-coated microwires, paying attention on amorphous and crystalline microwires.

3.1. Effect of magnetoelastic anisotropy on magnetic properties of amorphous glass-coated microwires

Magnetic properties of amorphous microwires are affected by the value and sign of the magnetostriction coefficient since the magnetoelastic interactions are the main source of the magnetic anisotropy of amorphous materials. The easiest way to tune the magnetostriction constant λ_s in amorphous alloys is the modification of its chemical composition [54-57].

Indeed, Fe-rich compositions possess positive λ_s –values, typically $\lambda_s \sim(20\text{-}40)\text{x}\cdot10^{-6}$, while for the Co-rich alloys the magnetostriction is negative ranging as $\lambda_s \sim\text{-}(5\text{-}3)\text{x}10^{-6}$ [56,57]. Accordingly, the magnetostriction can take vanishing values in Co-Fe or Co-Mn amorphous alloys on Co-rich side [54-58]. Alternatively, the decrease in λ_s is observed in Fe-Ni alloys with increasing Ni content. However, Ni doping correlates to the simultaneous decreasing of the saturation magnetization. Thus, zero λ_s at high Ni-content corresponds to paramagnetic ordering at room temperature [57].

The influence of the λ_s values and sign on hysteresis loops of amorphous microwires is shown in Figure 1.

As can be appreciated from Figure 1, the character of hysteresis loops for amorphous microwires with positive and negative λ_s –values is rather different: amorphous microwires with positive λ_s –values present rectangular hysteresis loops, while hysteresis loops of microwires with negative λ_s –values are almost non-hysteretic with low coercitivity, H_c, values.

Peer-reviewed version available at Processes 2020, 8, 1006; doi:10.3390/pr8081006

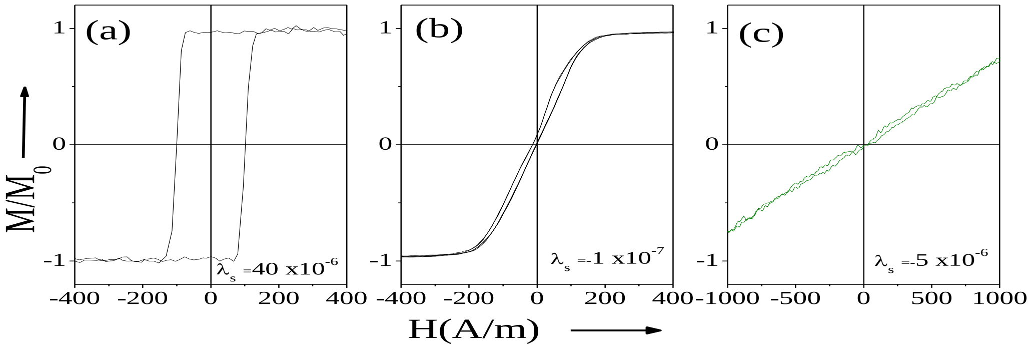

Figure 1. Hysteresis loops of magnetic microwires $Fe_{75}B_9Si_{12}C_4$ with positive (a) $Co_{67.1}Fe_{3.8}Ni_{1.4}Si_{14.5}B_{11.5}Mo_{1.7}$ with vanishing (b) and $Co_{77.5}Si_{15}B_{7.5}$ with negative (c) λ_s values. (Reproduced with permission from [42] Open Access Copyright © 2019 MDPI)

Such difference in hysteresis loops character is commonly attributed to different magnetic anisotropy of microwires with positive and negative λ_s –values: the rectangular hysteresis loop of microwires with positive λ_s –values was interpreted in terms of axial magnetic anisotropy [42]. Such axial magnetic anisotropy is intrinsically related to a peculiar domain structure consisting of inner axially magnetized single domain responsible for observation of the single and large Barkhausen jump and outer domain shell with radial magnetization orientation [9,59,60]. The remagnetization of such microwires is running by the depinning of the reversed domains inside the inner single domain and the consequent domain wall propagation [9,52,59-61]. Perfectly, rectangular shape of the hysteresis loop is related to an extremely high velocity of such domain wall propagation.

On the other hand, the origin of quasi-linear hysteresis loops (see Figures 1b,c) is related to the quasi-reversible magnetization rotation from the circumferential to the axial upon application of an axial magnetic field [60].

As regarding the aforementioned magnetoelastic anisotropy, K_{me}, another relevant parameter is the internal stresses value, σ_i. Indeed, K_{me} is given by [23,38,62-64]:

$$K_{me} \approx 3/2\lambda_s\sigma_i \qquad (2)$$

where total stresses, $\sigma = \sigma_i + \sigma_{app}$, σ_{app} - applied stresses.

There are several factors responsible for the internal stresses value and distribution: i) the difference in the thermal expansion coefficients of metallic alloy nucleus solidifying simultaneously with the glass coating surrounding it; ii) the quenching stresses itself related to the rapid solidification of the metallic alloy nucleus from the surface inside the wire axis; and iii) the drawing stresses [43-46,62-64].

Most theoretical evaluations of the internal stresses value and distribution show that the largest internal stresses are associated with the difference in the thermal expansion coefficients of the metallic alloy and the glass coating [62-64]. The quenching stresses are roughly an order of magnitude lower [42,43].

There are only several attempts of evaluation of internal stresses associated to the continuous mechanical drawing [63,64]. The value of such stresses has been estimated from the results on remanent magnetization measurements in glass-coated microwires with partially removed (by chemical etching) glass-coating under applied tensile stresses [63,64]. The value of this stress component depends on the microwire geometry and was estimated to be about 250-600 MPa, i.e., again about an order of magnitude below the internal stresses related to the difference in the thermal expansion coefficients of metallic alloy and the glass coating [63,64]. Furthermore, they further enhance the axial internal stresses arising from the difference in the thermal expansion coefficients of the metallic alloy and the glass coating.

Provided description allows to predict that the internal stresses value inside the metallic nucleus can be tuned by the ρ-ratio between the metallic nucleus diameter, d, and the total microwire diameter,

Peer-reviewed version available at Processes 2020, 8, 1006; doi:10.3390/pr8081006

D (ρ=d/D) [42,43,62-64]. In fact, this prediction is confirmed experimentally by correlation of magnetic properties, such as coercivity, H_c, or magnetic anisotropy field, H_k, in magnetic microwires of various chemical compositions and ρ -ratio [38,42,43,62-64]. Below we provide several experimental evidences of such correlations.

The influence of controllable glass-coating removal by etching in 10% HF on hysteresis loops of $Co_{70.5}Mn_{4.5}Si_{10}B_{15}$ microwire is shown in Figure 2. Gradual transformation of hysteresis loops from linear to almost perfectly rectangular must be attributed to relaxation of the internal stresses related to the presence of glass-coating. This evolution of hysteresis loops can be understood considering the low negative λ_s –values and the axial character of internal stresses in most part of the metallic nucleus [65]. Evident difference in hysteresis loops of as-prepared $Co_{70.5}Mn_{4.5}Si_{10}B_{15}$ microwires and microwires of the same composition with partially removed glass-coating experimentally confirms the aforementioned theoretical results on character of internal stresses. Low negative magnetostriction coefficient and preferentially axial character of internal stresses explain linear almost non-hysteretic character of hysteresis loops of as-prepared $Co_{70.5}Mn_{4.5}Si_{10}B_{15}$ microwires.

The influence of chemical etching on the hysteresis loops of $Co_{68.5}Si_{14.5}B_{14.5}Y_{2.5}$ microwire with higher negative λ_s –values is even more remarkable (see Figure 3): as-prepared $Co_{68.5}Si_{14.5}B_{14.5}Y_{2.5}$ microwire presents non-hysteretic loops with saturation at magnetic field, H, above 6 kA/m (see Figure 3a). However, upon chemical etching gradual transformation of hysteresis loops from linear to rectangular is observed (see Figures 3b,c). As previously reported [66], after etching in 10% HF for 50 min the glass-coating thickness decreases from 8.5 to 4 μm. Accordingly, the glass-coating thickness can be considered as one of the most relevant parameters that affect the hysteresis loops of glass-coated microwires.

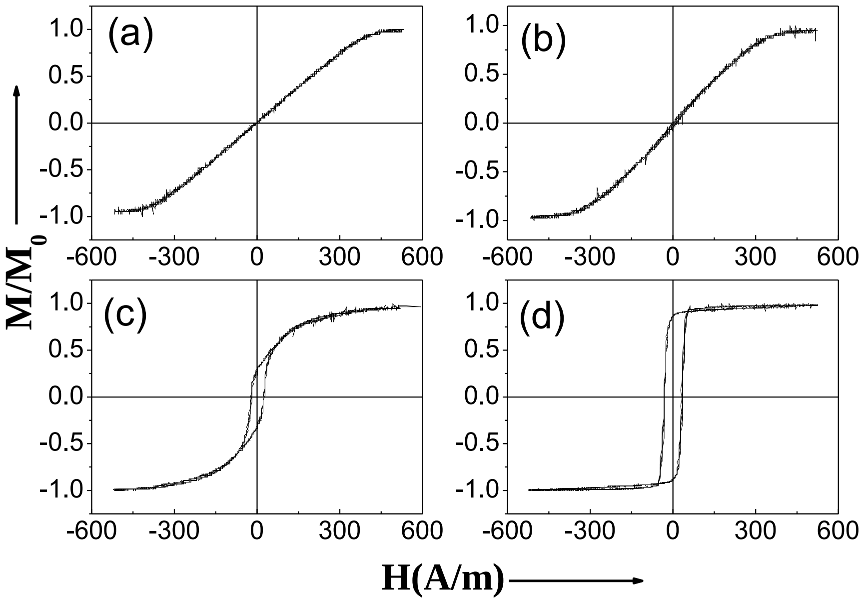

Figure 2. Hysteresis loops of as-prepared (a) and with chemically etched glass-coating for 5 min (b), 10 min (c) and 50 min (c) $Co_{70.5}Mn_{4.5}Si_{10}B_{15}$ microwire. (Reproduced with permission from [65], Fig.5. Copyright © 2000 Elsevier)

Gradual glass-coating removal by chemical etching must be associated to the gradual relaxation of the internal stresses related to different thermal expansion coefficients of metallic alloy and glass coating.

The commonly accepted model of domain structure of magnetic wires is the core-shell model experimentally proved several times by various methods [60,61,67,68]. In according to this model the domain structure of amorphous magnetic wires can be satisfactory described as consisting of inner axially magnetized core surrounded with the outer shell with transverse magnetization. In the

Peer-reviewed version available at Processes 2020, 8, 1006; doi:10.3390/pr8081006

case of Fe-rich wires the outer shell presents radial magnetization orientation, while in Co-rich microwires bamboo-like domain structure with circular magnetization orientation is reported [60,61,67-70].

The origin for such domain structure is discussed considering the minimization of the energy though the counterbalance of the magnetoelastic energy related to the internal stresses distribution as well as to the exchange energy [69,70].

In the frame of this domain structure model the radius of the inner axially magnetized core, R_c, can be evaluated from the squareness ratio, M_r/M_o, as:

$$R_c = R(M_r/M_o)^{1/2} \qquad (3)$$

where R is the metallic nucleus radius.

From the evolution of the hysteresis loops upon chemical etching provided in Figures 2&3, the increase in the M_r/M_o upon chemical etching is evidenced. Consequently, we can assume that the radius of inner axially magnetized domain increase upon partial internal stresses relaxation associated to the glass removal. This assumption is evidenced from Figure 4 where evolution of R_c/R on time of chemical etching, t, for $Co_{70.5}Mn_{4.5}Si_{10}B_{15}$ and $Co_{68.5}Si_{14.5}B_{14.5}Y_{2.5}$ microwires is shown. As can be observed, for the microwire with lower λ_s –value the increase in R_c/R with t is faster.

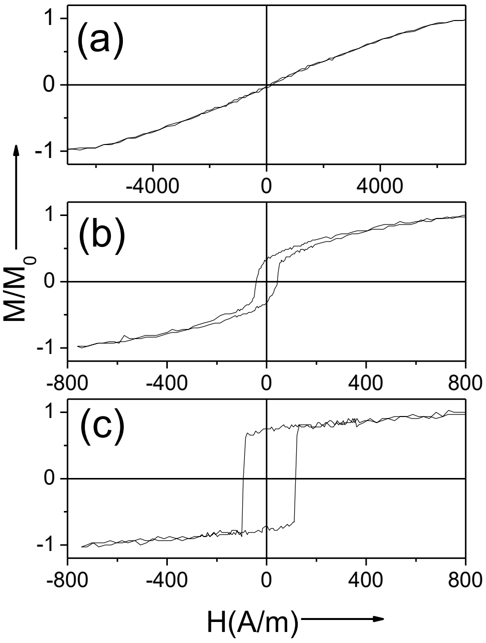

Figure 3. Hysteresis loops of as- prepared (a), and subjected to chemical etching for 35 min (b) and 50 min (c) $Co_{68.5}Si_{14.5}B_{14.5}Y_{2.5}$ microwires. Adapted from [66].

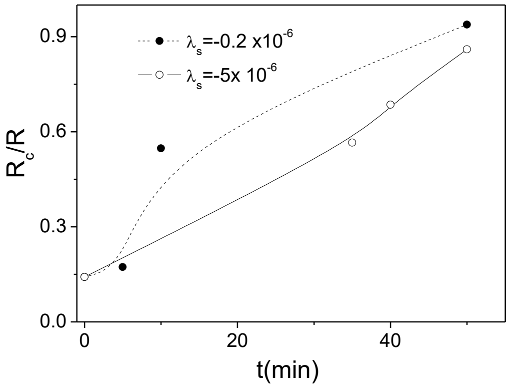

Figure 4. R_c/R (t) dependencies for $Co_{70.5}Mn_{4.5}Si_{10}B_{15}$ and $Co_{68.5}Si_{14.5}B_{14.5}Y_{2.5}$ microwires. The lines are just guides for eyes.

In order to prove the axial character of the internal stresses related to glass-coating (i.e., to the difference in thermal expansion coefficients of glass and metallic alloy) we evaluated the influence of applied tensile stresses, σ, on the hysteresis loops of Co-rich ($Fe_{3.8}Co_{65.4}Ni_{1}B_{13.8}Si_{13}Mo_{1.35}C_{1.65}$) microwires with linear hysteresis loop.

As shown in Figure 5a, when tensile stress, σ_{app}, is applied, magnetic anisotropy field, H_k, increases. At the same time, the hysteresis loops character (linear hysteresis loop with low coercivity) of the studied microwire remains almost the same.

$H_k(\sigma_{app})$ dependence evaluated from Figure 5a shows a good linear tendency (Figure 5b). Such linear $H_k(\sigma_{app})$ dependence has been explained considering the relationship between the magnetoelastic anisotropy, K_{me}, and σ_{app} given by eq. (2) [71]. Consequently, relation between the magnetostriction coefficient and magnetic anisotropy field, H_k, is given by [71]:

$$\lambda_s = \mu_o M_s (H_k/3\sigma) \qquad (4)$$

Peer-reviewed version available at *Processes* **2020**, *8*, 1006; doi:10.3390/pr8081006

where $\mu_o M_s$ is the saturation magnetization.

The magnetostriction coefficient is affected by the stresses, σ, as described elsewhere [71,72]:

$$\lambda_{s,\sigma} = \lambda_{s,0} - B\sigma \qquad (5)$$

where $\lambda_{s,\sigma}$ is the magnetostriction coefficient under stress, $\lambda_{s,,0}$ is the zero-stress magnetostriction constant and B is a positive coefficient of order 10^{-10} MPa and $\sigma-$ stresses. Therefore, a decrease in λ_s reported for Co-rich microwires ($\lambda_s<0$) upon applied stresses [54,55] can be associated with the development of circumferential magnetic anisotropy in the outer shell [71]. Consequently, experimentally observed linear $H_k(\sigma_{app})$ dependence can be explained considering eqs. (2,4, 5).

The influence of chemical etching on the hysteresis loops and on H_k observed in Figures 2, 3 is exactly the opposite to the effect of tensile stresses. Therefore, the theoretically predicted character of internal stresses with a dominant axial tensile character and its dependence on the ρ-ratio look reasonable. Accordingly, it is expected that the internal stresses value can be tuned by the glass-coating thickness through the ρ–ratio.

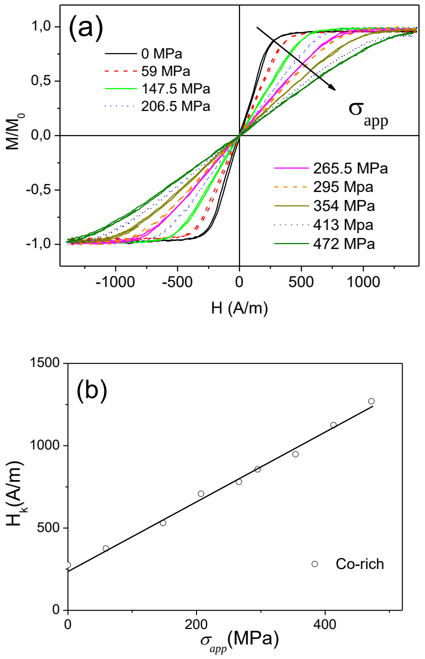

Figure 5. Effect of applied stress on hysteresis loops (a) and $H_k(\sigma_{app})$ (b) for as-prepared $Fe_{3.8}Co_{65.4}Ni_1B_{13.8}Si_{13}Mo_{1.35}C_{1.65}$ microwires. (Reproduced with permission from [71] Fig2, Fig.3a Copyright © 2019 Elsevier B.V).

The correlation of the ρ–ratio and the hysteresis loops of Co-rich microwires with a vanishing magnetostriction coefficient is reported elsewhere [12,73-75]. For the case of $Co_{67}Fe_{3.85}Ni_{1.45}B_{11.5}Si_{14.5}Mo_{1.7}$ microwires with vanishing magnetostriction coefficient (see Figure 6) linear almost non-hysteretic loops with extremely low coercivities (up to 4 A/m) are observed. If we plot H_k obtained from the hysteresis loops of $Co_{67}Fe_{3.85}Ni_{1.45}B_{11.5}Si_{14.5}Mo_{1.7}$ microwires with various d and D-values versus the ρ–ratio, we can find out that there is a correlation between these parameters. Magnetic anisotropy field, H_k, increases with decreasing the ρ–ratio (Figure 6b).

As mentioned above, glass-coated microwires with positive λ_s –value generally present perfectly rectangular hysteresis loops related to spontaneous magnetic bistability. Typical hysteresis loop of microwires with positive λ_s –value is shown in Figure 1a. Fast magnetization switching and related single DW propagation reported in magnetic micro- and nano-wires are proposed for various technical applications, like magnetic sensors, electronic surveillance, magnetic memories and logics [7,75-77]. Thus, the method for magnetic codification using magnetic tags [75] is based on sharp voltage signals induced by fast magnetization switching of magnetically bistable microwires. In this application, each tag contains several microwires with well-defined coercivities, each of them characterized by a rectangular hysteresis loop. Once the magnetic tag submitted to the AC magnetic field, each particular microwire is remagnetized at different magnetic field giving rise to an electrical signal on a detecting system. Variety of coercivities allows to extend the number of combinations for magnetic codification. Therefore, tunability of coercivities, H_c, of magnetically bistabile microwires is essentially relevant for this application and has been extensively studied [46,78-80].

Peer-reviewed version available at Processes 2020, 8, 1006; doi:10.3390/pr8081006

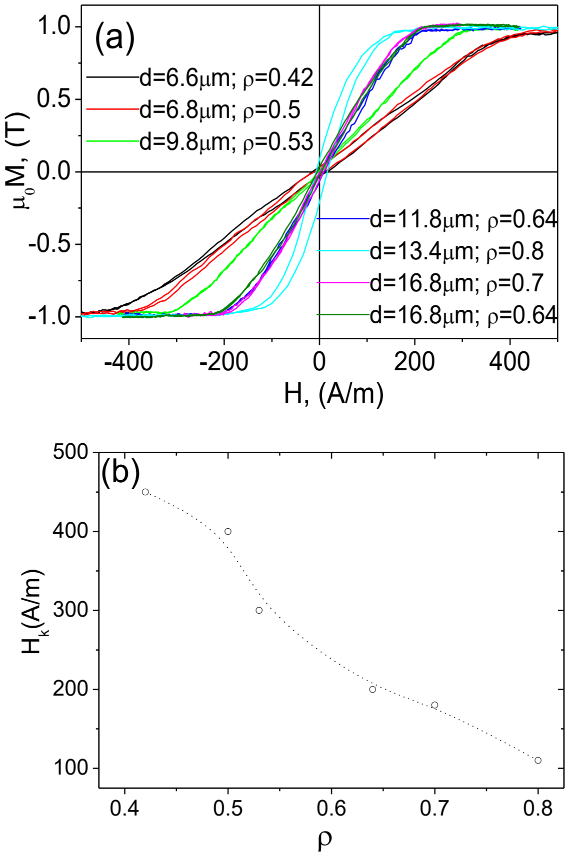

Figure 6. Hysteresis loops of $Co_{67.1}Fe_{3.8}Ni_{1.4}$ $Si_{14.5}$ $B_{11.5}Mo_{1.7}$ microwires with different geometry (a) and $H_k(\rho)$ dependence for the same microwires. (Reproduced with permission from [12] Fig7 Copyright © 2015 Elsevier B.V).

As can be appreciated from Figure 7, even for the same microwire composition, H_c can be changed by almost an order of magnitude (from 85 to 630 A/m) by adjusting the ρ-ratio. Similarly to the case of Co-rich microwires, H_c-values obtained for microwires with different D and d –values can be represented by $H_c(\rho)$ dependence (i.e. H_c –values for different D and d -values can be represented by $H_c(\rho)$ dependence, (see Figure 7e).

Considering aforementioned results, one can expect that stresses relaxation by heat treatment can efficiently affect the magnetic properties of microwires.

One of the examples of annealing influence on hysteresis loops of Fe-rich microwires is shown in Figure 8.

For the $Fe_{75}B_9Si_{12}C_4$ microwires, annealing does not affect the hysteresis loop character. However, a slight H_c decrease is observed (see Figure 8b).

More complex behavior has been reported for Fe-Ni based microwires with positive magnetostriction and hence presenting spontaneous magnetic bistability [81,82].

As-prepared $Fe_{62}Ni_{15.5}Si_{7.5}B_{15}$ microwires present rectangular hysteresis loops (see Figure 9a) as expected for microwires with positive λ_s –values

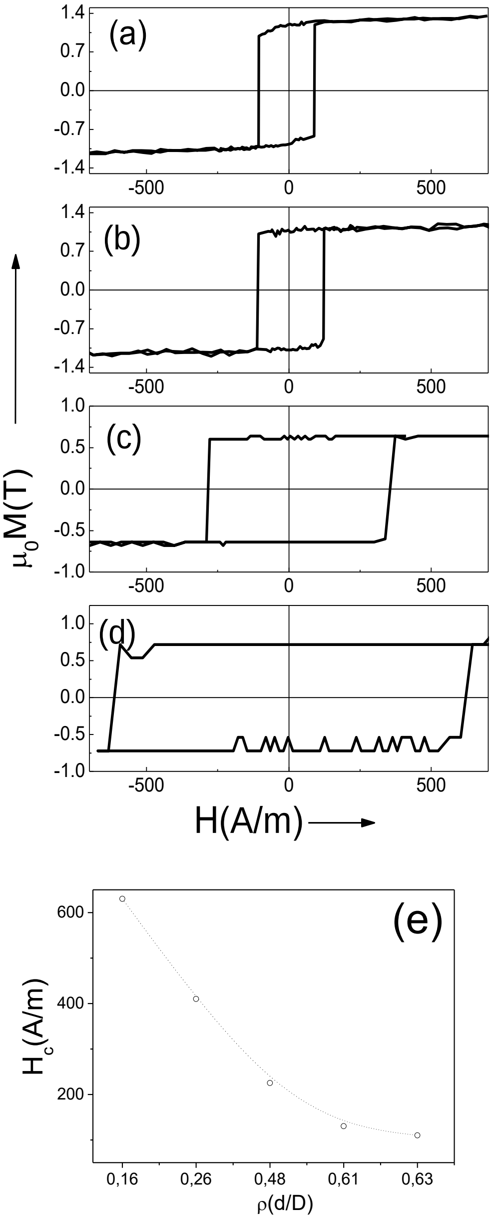

Figure 7. Hysteresis loops of $Fe_{70}B_{15}Si_{10}C_5$ amorphous microwires with different metallic nucleus diameter *d* and total diameters *D*: with ρ = 0.63; *d*=15 μm (a);ρ= 0,48; *d*= 10,8 μm (b); ρ =0,26; *d*= 6 μm (c); ρ =0,16; *d*= 3 μm (d) and $H_c(\rho)$ dependence of the same microwires. Adapted from [78].

(about 27 x10^{-6}).

After annealing, an increase in coercivity, H_c, is generally observed (see Figure 9 b-g and Figure 10). The hysteresis loop character remains unchanged: all hysteresis loops present rectangular shape.

Although generally higher H_c -values are observed in annealed samples, $H_c(t_{ann})$ dependence is not monotonic: for t_{ann}, =128 min some H_c decrease is observed (see Figure 10).

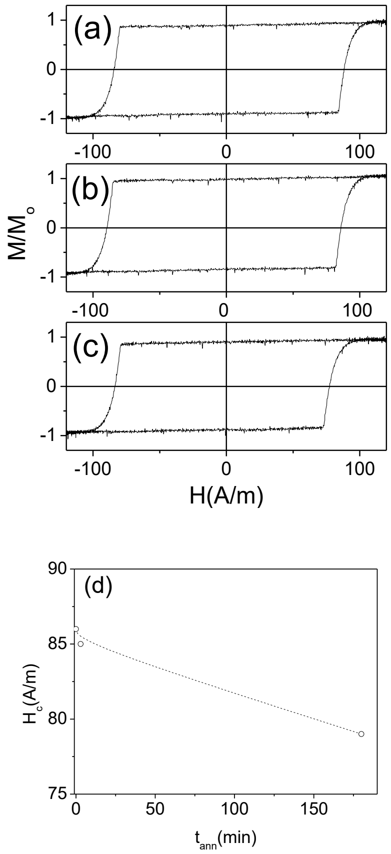

Figure 8. Hysteresis loops of as-prepared (a), and annealed at T_{ann}= 400 °C for 3 min (b) and 180 min (c) $Fe_{75}B_9Si_{12}C_4$ microwires and dependence of coercivity on annealing time (d).

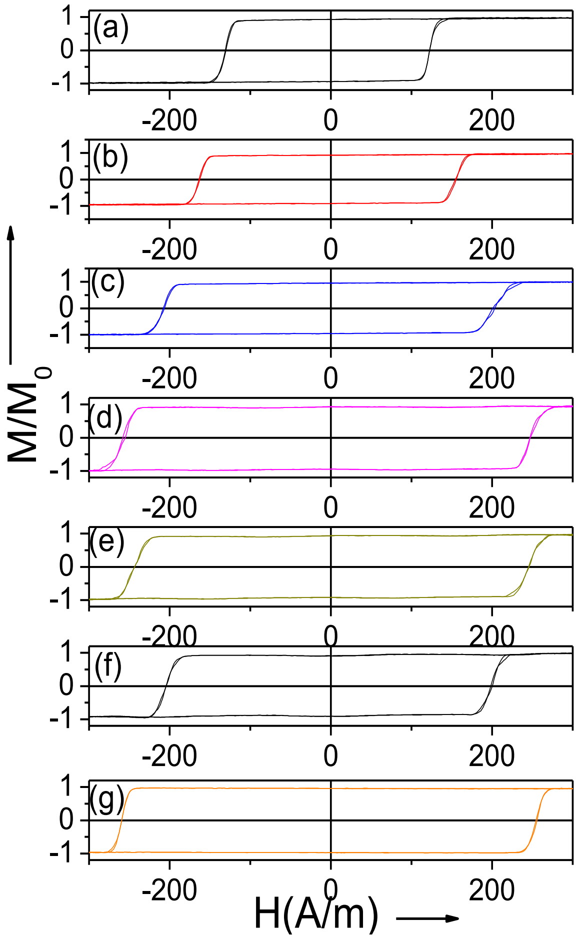

Figure 9. Hysteresis loops of as-prepared (a) and annealed at T_{ann}=410 °C for 4 min (b), 16 min (c) 32 min (d), 64 min (e), 128 min (f) and 256 min (g) $Fe_{62}Ni_{15.5}Si_{7.5}B_{15}$ microwires. Adapted from [81].

Similarly, the second Fe-Ni based ($Fe_{49.6}Ni_{27.9}Si_{7.5}B_{15}$) microwire presents rectangular hysteresis loops in as-prepared state and after annealing (see Figure 11). Lower H_c –values observed in as-prepared $Fe_{49.6}Ni_{27.9}Si_{7.5}B_{15}$ microwire can be related to lower λ_s –values of $Fe_{49.6}Ni_{27.9}Si_{7.5}B_{15}$ microwires (λ_s ≈20 x10^{-6}) [54,55]. However, $H_c(t_{ann})$ dependence is different from that showed by $Fe_{62}Ni_{15.5}Si_{7.5}B_{15}$ microwire: upon annealing (at the same

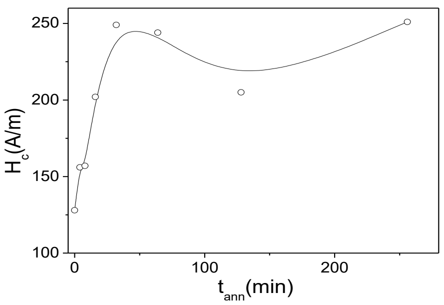

Figure 10. $H_c(t_{ann})$ dependence evaluated in $Fe_{62}Ni_{15.5}Si_{7.5}B_{15}$ microwires. (Reproduced with permission from [81] Fig 2d Copyright © 2020 AIP Publishing LLC, Open Access)

Peer-reviewed version available at Processes 2020, 8, 1006; doi:10.3390/pr8081006

conditions, i.e., T_{ann} and t_{ann}) first a slight decrease in H_c followed by H_c rising is observed (see Figure 11e).

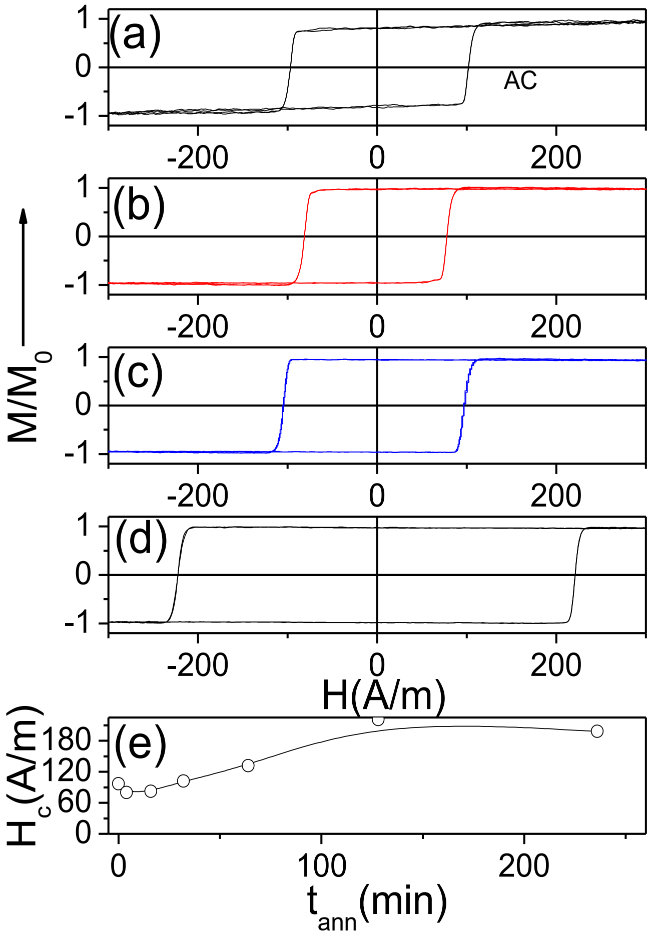

Figure 11. Hysteresis loops of as-prepared (a) and annealed at T_{ann}=410 °C for t_{ann}= 4 min (b) 32 min(c) 128 min (d) and $H_c(t_{ann})$ dependence (e) for $Fe_{49.6}Ni_{27.9}Si_{7.5}B_{15}$ microwires. (Reproduced with permission from [81] Fig 4 Copyright © 2020 AIP Publishing LLC, Open Access)

Considering that the annealing is the common route for the internal stresses relaxation, observed annealing effect on H_c in Fe-Ni microwires looks unexpected. For explanation of rather different effect of annealing on coercivity of Fe and Fe-Ni based microwires different factors such as beginning of crystallization process or domain wall stabilization due to directional ordering of atomic pairs are considered [81-84]. From our previous studies we must disregard the crystallization process, since Fe-Ni based microwires annealed at the same T_{ann} for 8 hours still present amorphous structure [85]. Therefore, observed $H_c(t_{ann})$ dependencies must be attributed to the changes in local atomic environment within the amorphous structure related to annealing. Thus, local nano-sized precipitations have been observed in annealed Fe-Ni based microwires by the atom probe tomography [85].

Furthermore, atom pair ordering and hence DW stabilization is reported for Fe-Ni and Fe-Co amorphous alloys [81-84,86,87].

Such DW stabilization is considered as the main origin of the H_c rising upon annealing observed in amorphous materials containing two or more ferromagnetic elements [88,89]. Such magnetic hardening is usually reported for annealing temperature below Curie temperature, T_c. This mechanism can explain the difference in annealing influence on coercivity in Fe- based and Fe-Ni based microwires. In addition, the Curie temperature, T_c, of $Fe_{49.6}Ni_{27.9}Si_{7.5}B_{15}$ amorphous alloys is about 400 °C, being considerably lower than that for $Fe_{62}Ni_{15.5}Si_{7.5}B_{15}$ alloy [90]. Accordingly, the DW stabilization for $Fe_{62}Ni_{15.5}Si_{7.5}B_{15}$ microwire is expected to be more relevant than that for $Fe_{49.6}Ni_{27.9}Si_{7.5}B_{15}$ microwire and hence the internal stresses relaxation plays a major role in the alloy with lower T_c.

Additionally, chemical composition of $Fe_{49.6}Ni_{27.9}Si_{7.5}B_{15}$ microwire is similar to the Invar-like composition (Ni/Fe content about 40/60) [82]. The peculiarity of the Invar-like crystalline materials with Ni/Fe content about 40/60 is that they can present the Invar anomaly, i.e., low thermal

Peer-reviewed version available at Processes 2020, 8, 1006; doi:10.3390/pr8081006

expansion coefficient [91]. The Invar anomaly is intrinsically related to the local atomic structure of Fe-Ni alloys. Considering similarity of short range order of amorphous and crystalline materials [92] one can expect lower internal stresses influence in $Fe_{49.6}Ni_{27.9}Si_{7.5}B_{15}$ microwire. In spite of observed magnetic hardening of Fe-Ni based microwires upon annealing, observed experimental dependencies allows to tune the coercivity value by annealing.

Even more remarkable hardening upon conventional annealing has been reported in variety of Co-rich microwires with vanishing λ_s –values [49,93]. Thus, considerable magnetic hardening and transformation of linear hysteresis loop with low coercivity ($H_c \approx 4$ A/m) into rectangular with $H_c \approx 90$ A/m upon annealing without stress is observed in $Fe_{3.6}Co_{69.2}Ni_{1}B_{12.5}Si_{11}Mo_{1.5}C_{1.2}$ microwire (see Figure 12). Gradual squareness ratio, M_r/M_o, rising upon T_{ann} increasing can be appreciated, although $Fe_{3.6}Co_{69.2}Ni_{1}B_{12.5}Si_{11}Mo_{1.5}C_{1.2}$ microwires annealed at different T_{ann} present similar coercivity.

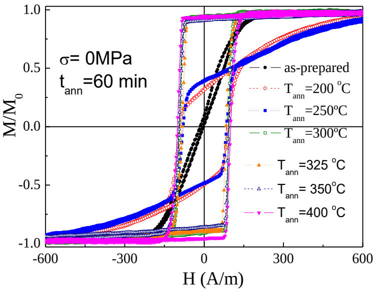

Figure 12 Hysteresis loop of the $Fe_{3.6}Co_{69.2}Ni_{1}B_{12.5}Si_{11}Mo_{1.5}C_{1.2}$ microwires annealed without stress at different temperatures. (Reproduced with permission from [49] Fig3a Copyright © 2020 Elsevier B.V)

Observed behavior of M_r/M_o upon annealing must be attributed to rising of the inner axially magnetized inner core diameter. Using relation (3) between the radius of the inner axially magnetized core, R_c, and M_r/M_o, one can obtain $R_c(T_{ann})$ dependence (see Figure 13). Observed modification of the hysteresis loops shape and obtained $R_c(T_{ann})$ dependence are consistent with the evolution of the hysteresis loop shape upon glass-coating removal by chemical etching (see Figures 3,4). Accordingly, $R_c(T_{ann})$ dependence and observed evolution of the hysteresis loops upon annealing must be related to the relaxation of internal stresses as discussed elsewhere [74, 93-95]

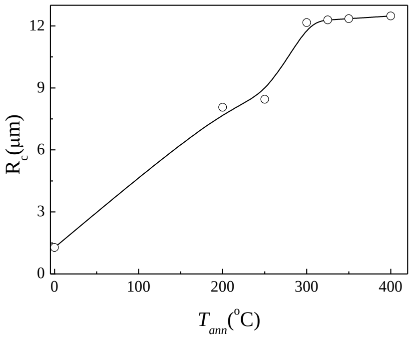

Figure 13. Dependence of radius of inner axially magnetized core, R_c, on annealing temperature, T_{ann}, in studied microwire. (Reproduced with permission from [49] Fig4 Copyright © 2020 Elsevier B.V)

Such evolution of hysteresis loops upon annealing is confirmed in various Co-based microwires with low and negative λ_s –values [93-96]. One more example for another Co-rich ($Co_{69.2}Fe_{4.1}B_{11.8}Si_{13.8}C_{1.1}$) microwire with low negative λ_s –values is shown in Figure 14. In this case the annealing temperature was fixed (T_{ann} =250 °C) and the hysteresis loops have been recorded at different annealing time, t_{ann}. Similarly to the case of $Fe_{3.6}Co_{69.2}Ni_{1}B_{12.5}Si_{11}Mo_{1.5}C_{1.2}$ microwires, we can observe a remarkable H_c rising and gradual M_r/M_o, increase with an increase in t_{ann} (see Figure 15). Accordingly, from $R_c(t_{ann})$ evaluated from M_r/M_o we can again observe gradual increase of the inner axially magnetized domain radius upon annealing.

Consequently, similarly to glass-coating removal, annealing of Co-rich microwires allows to obtain magnetically bistable Co-rich microwires. Such Co-rich microwires with magnetic bistability induced by annealing present fast magnetization switching by propagation of single domain wall,

Peer-reviewed version available at Processes 2020, 8, 1006; doi:10.3390/pr8081006

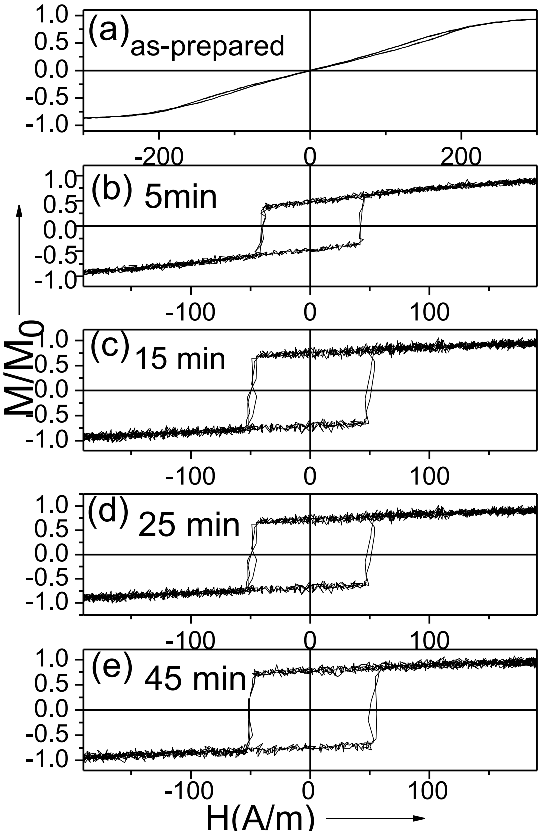

Figure 14. Effect of annealing time on hysteresis loops of Co$_{69.2}$Fe$_{4.1}$B$_{11.8}$Si$_{13.8}$C$_{1.1}$ microwires annealed at T_{ann} =250 °C. Adapted from [96] Fig. 2 Copyright © 2014 Springer Nature.

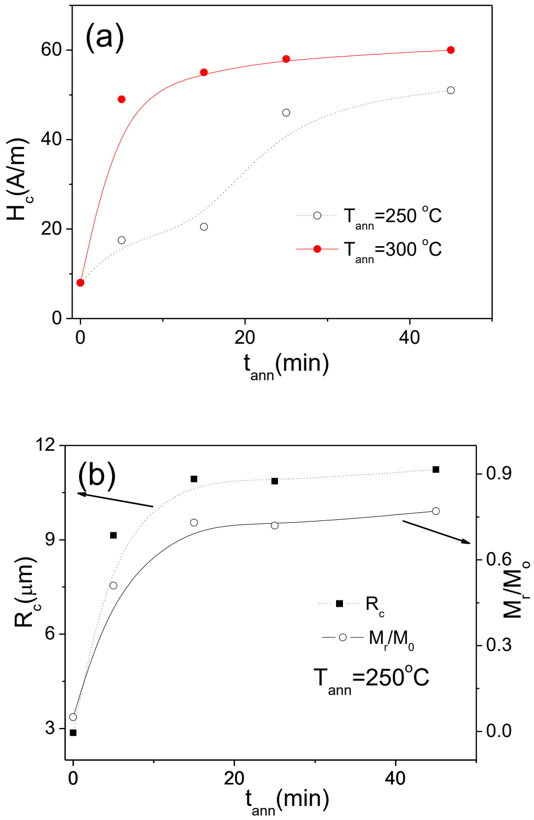

Figure 15. Dependence of coercivity, H_c, (a) and reduced remanent magnetization, M_r/M_{Hmax} (b) on annealing time, t_{ann} in Co$_{69.2}$Fe$_{4.1}$B$_{11.8}$Si$_{13.8}$C$_{1.1}$ microwires. Adapted from [96] Fig. 4 Copyright © 2014 Springer Nature.

similarly to Fe-rich microwires [60]. However, magnetic properties of either annealed or chemically etched Co-rich microwires are similar to those of Fe-rich microwires: the coercivity values of either annealed or chemically etched Co-based microwires are almost an order of magnitude higher than those of as-prepared Co-based microwires.

Therefore, optimization of the magnetic softness of amorphous microwires requires development of special post-processing. One of the promising routes allowing achievement of better magnetic softness is controllable magnetic anisotropy induction. Below we will present several examples of thermal treatment allowing magnetic properties optimization of magnetic microwires.

3.2. Effect of induced magnetic anisotropy on hysteretic magnetic properties of amorphous glass-coated microwires

Considering new functional properties provided by insulating and flexible glass-coating, most attention has been paid to tuning of the hysteresis loops of Fe-Co-Ni- based microwires by appropriate annealing. As shown above, conventional annealing provides limited possibilities for tuning the hysteresis loops. Accordingly, several attempts have been performed recently to search more efficient post-processing allowing tuning the magnetic properties [43,52, 97].

Peer-reviewed version available at Processes 2020, 8, 1006; doi:10.3390/pr8081006

One of the most promising and effective methods for tuning of the magnetic properties of magnetic microwires is stress-annealing. In the case of magnetic microwires with positive magnetostriction coefficient, this post-processing allows remarkable magnetic softness improvement [43,52,86,87,94,95].

From previous knowledge on the origin of induced magnetic anisotropy, it is known that the magnetic anisotropy of amorphous materials can be effectively tailored by either stress or magnetic field annealing [83,84].

Recently, stress-annealing has been successfully employed for tailoring of magnetic properties in glass-coated microwires. Thus, according to several publications on the origin of the induced anisotropy in glass-coated microwires [74,86,87,98] the presence of the glass-coating can be even beneficial for tuning the magnetic anisotropy.

Several examples on the influence of stress-annealing on magnetic properties of glass-coated microwires are provided below.

From Figure 16 we can clearly see that stress-annealing performed at the same conditions (T_{ann} and t_{ann}) allows better magnetic softening and transverse anisotropy induction in Fe-based ($Fe_{75}B_9Si_{12}C_4$) microwire. As reported elsewhere [87,98], such transverse anisotropy depends on various parameters, like T_{ann}, t_{ann}, and stress, σ_m, applied during the annealing [87]. Clear example is shown in Figure 17. As can be appreciated from Figure 17, for high enough T_{ann} or σ_m a remarkable transverse magnetic anisotropy can be induced.

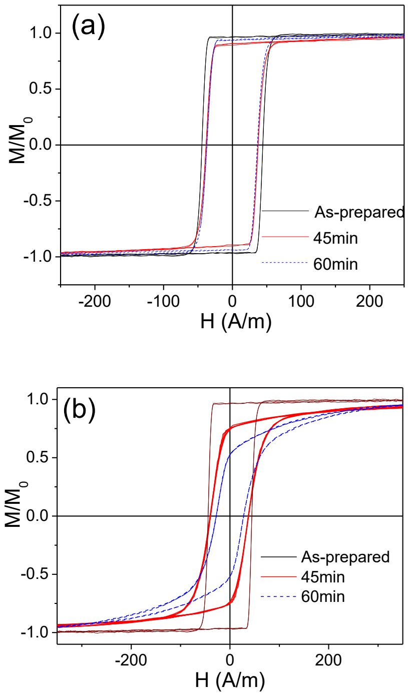

Figure 16. Hysteresis loops of as-prepared and annealed at T_{ann} = 325 °C (a) and as-prepared and stress- annealed at T_{ann} = 325 °C and σ_m=190 MPa (b) $Fe_{75}B_9Si_{12}C_4$ microwire. Adapted from [98].

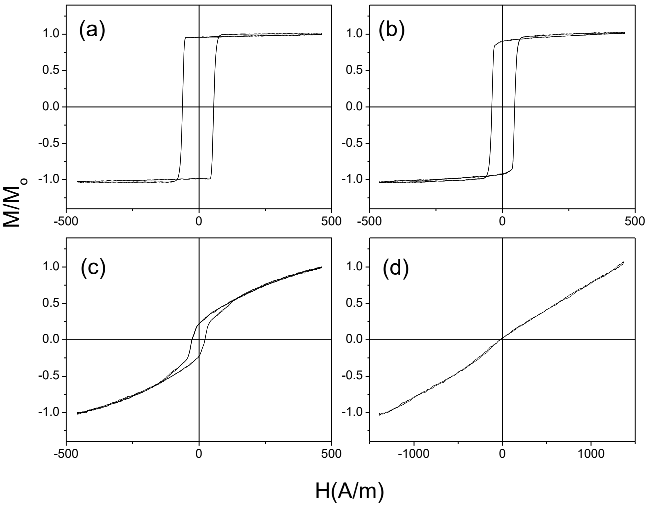

Figure 17. Hysteresis loops of as-prepared (a), annealed at 200 °C (b), 250 °C (c) and 300 °C (d) for 1 h and σ_m ≈900 MPa $Fe_{75}B_9Si_{12}C_4$ microwires. (Reproduced with permission from [87] Fig 1 Copyright © 2018, Springer Nature, Open Access)

However, for low enough T_{ann}, t_{ann} or σ_m the hysteresis loops maintain rectangular shape (see Figure 18a) and can present all the features typical for magnetically bistable microwires, i.e., fast and single domain wall propagation [98]. Lower coercivity is generally observed in stress-annealed Fe-rich microwires (see Figure 18a,b). Consequently, stress annealing allows more effectively tune H_c and M_r/M_o –values (see Figure 18c). However, for sufficiently high T_{ann}, t_{ann} or σ_m the hysteresis loops of Fe-rich microwires become inclined (similar to that of as-prepared Co-rich microwires) with clear transverse magnetic anisotropy (see Figures 17d, 18b). As recently reported [42,43,86,87], such Fe-rich microwires with stress-induced transverse magnetic anisotropy present better GMI response

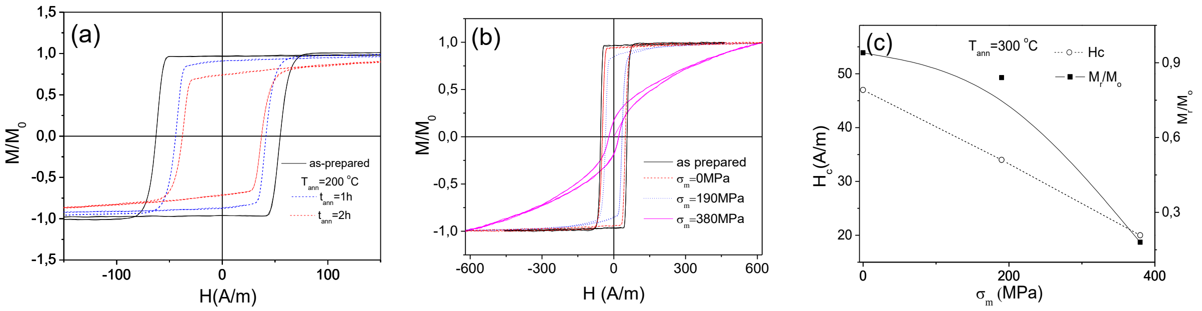

Figure 18. Hysteresis loops of as-prepared and stress-annealed at T_{ann}=200° C, σ≈900 MPa for different t_{ann}(a), effect of tensile stress applied during the annealing at T_{ann}=300° C on hysteresis loops (b) and H_c and M_r/M_o values (c) of $Fe_{75}B_9Si_{12}C_4$ microwires. Figures 18a is adapted from [87] Fig. 2 (Copyright © 2018, Springer Nature, Open Access)

as well as GMI effect and hysteresis loops sensitive to applied stresses [99,100]. Therefore, such microwires can be suitable for development of magnetic sensors based on GMI effect or for magnetoelastic sensors [32,71].

In the case of Co-based microwires higher annealing temperature, time or stresses are required to prevent magnetic hardening associated to relaxation of internal stresses related to glass-coating [42,43, 101]. As can be observed in Figures 19 and 20, for extended range of T_{ann}, t_{ann} or σ_m, stress-annealed Co-rich microwires present rectangular hysteresis loops. Therefore, stress-annealing of Co-rich microwires allows to tune their coercivity in quite extended range. Thus, at certain stress-annealing conditions $Co_{68.7}Fe_4Ni_1B_{13}Si_{11}Mo_{2.3}$ microwires with rectangular hysteresis loops and extremely low coercivity of about 1A/m can be obtained (see Figure 21) [102].

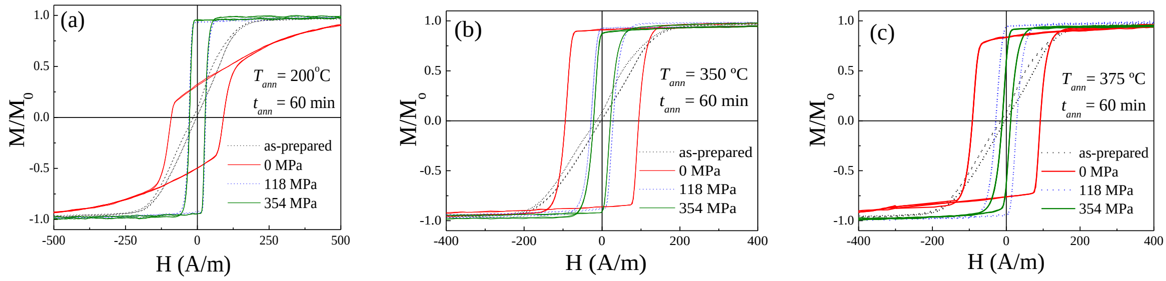

Figure 19. Hysteresis loops of $Fe_{3.6}Co_{69.2}Ni_1B_{12.5}Si_{11}Mo_{1.5}C_{1.2}$ microwires stress-annealed at different conditions. (Reproduced with permission from [49] Fig7 Copyright © 2020 Elsevier B.V).

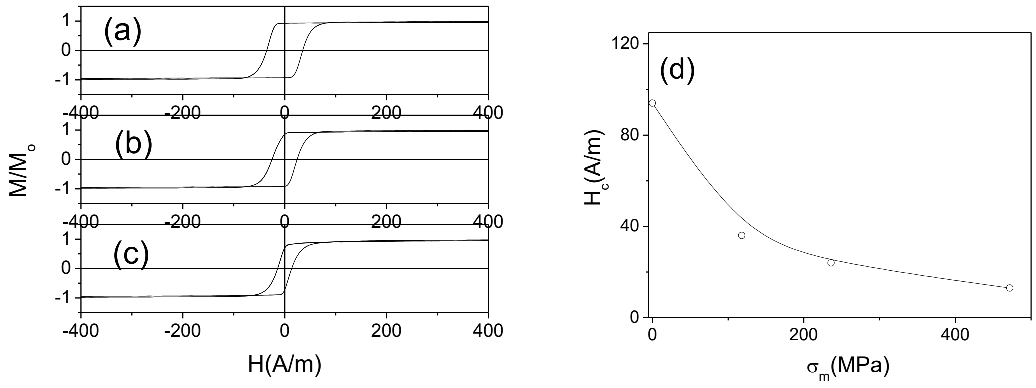

Figure 20. Hysteresis loops of $Fe_{3.6}Co_{69.2}Ni_1B_{12.5}Si_{11}Mo_{1.5}C_{1.2}$ microwires annealed at T_{ann}=300 °C for t_{ann}=1 h under σ_m=118 (a), σ_m=236 (b) and σ_m=472 MPa (c) and $H_c(\sigma_m)$ dependence at T_{ann}=300 °C for t_{ann}=1 h (d).

For sufficiently high T_{ann}, t_{ann} or σ_m-values linear hysteresis loop of $Fe_{3.6}Co_{69.2}Ni_1B_{12.5}Si_{11}Mo_{1.5}C_{1.2}$ microwires can be recovered (see Figure 19). However, T_{ann}, t_{ann} or σ_m-values at which transverse

Peer-reviewed version available at *Processes* **2020**, *8*, 1006; doi:10.3390/pr8081006

magnetic anisotropy in Co-rich microwires can be induced are considerably higher than those for Fe-rich microwires.

One more efficient method for tuning of hysteresis loops of Co-rich microwires, preventing excessive magnetic hardening, is the Joule heating (see Figure 22) [29]. In this case, the current flowing through the microwires produce heating itself as well as the circumferential magnetic field, H_{circ}, (associated to the current I flowing through the sample) [29,103].

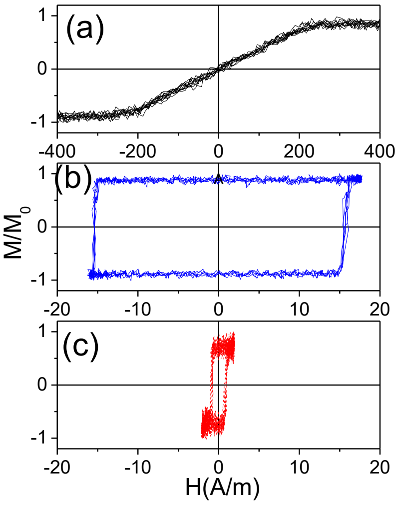

Figure 21. Hysteresis loops of as-prepared (a), annealed at T_{ann}=350° C (b) and stress annealed at T_{ann}=350° C and σ_m=250 MPa (c) $Co_{68.7}Fe_4Ni_1B_{13}Si_{11}Mo_{2.3}$ microwires. Adapted from ref [102].

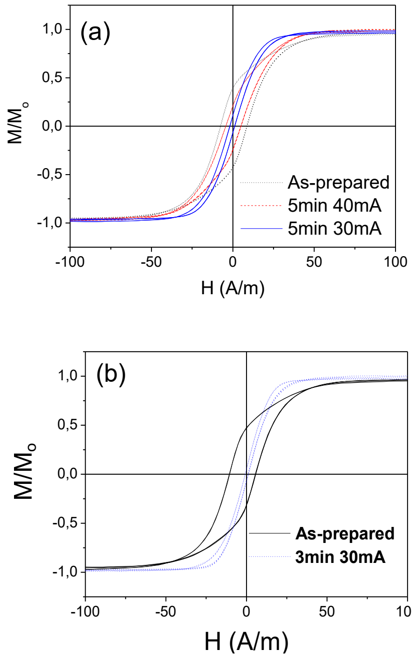

Figure 22. Hysteresis loops of as-prepared and current annealed at 30 mA and 40 mA for 5 min (a), 3 min and 30 mA (b) $Co_{67}Fe_{3.9}Ni_{1.5}B_{11.5}Si_{14.5}Mo_{1.6}$ amorphous glass-coated microwire. (Reproduced with permission from [26] Fig4 Copyright © 2019 Elsevier B.V)

Aforementioned circumferential magnetic field, H_{circ}, produced by the current (Oersted field) in the surface of the metallic nucleus can be evaluated from the formula [29,86]:

$$H_{circ}=I/2\pi r \qquad (6)$$

where I is the current value, r- radial distance.

Magnetic softening obtained at certain conditions of Joule heating is evidenced by Figure 22 where effect of Joule heating on hysteresis loops of $Co_{67}Fe_{3.9}Ni_{1.5}B_{11.5}Si_{14.5}Mo_{1.6}$ microwire is shown. In this case the microwires were heated by a DC current, I, of 30 and 40 mA. These conditions were selected in order to avoid the crystallization and related deterioration of the magnetic properties. In the case of Joule heating the current density is one of the main parameters determining the sample heating [104]. Although the thickness of the glass coating and the metallic nucleus diameter also affect the heat transfer rate [40]. In the given case, the current densities (58.3 and 77.7 A/mm^2 for 30 and 40 mA, respectively) are well-below the value that can produce magnetic hardening related to the crystallization [104].

Observed magnetic softening is related to the presence of magnetic field that can considerably affect the magnetic anisotropy of amorphous materials [105]. It was reported that the macroscopic magnetic anisotropy of amorphous materials is originated by a preferred magnetization direction during the annealing and was discussed in terms of either the directional ordering of atomic pairs or compositional and topological short-range ordering [83-85,93-95,105].

3.3. Tuning of hysteretic magnetic properties in crystalline and devitrified glass-coated microwires

Peer-reviewed version available at *Processes* **2020**, *8*, 1006; doi:10.3390/pr8081006

The devitrification of amorphous nucleus reached by post annealing process is another useful tool allowing considerable modification of the magnetic properties and even magnetic softening in some Fe-rich microwires [48].

In the case of FeSiBNbCu (so-called Finemet) alloys low magnetostriction values and better magnetic softness can be achieved by the devitrification of amorphous precursor [57]. Magnetic softening of Finemet alloys is commonly attributed to vanishing magnetocrystalline anisotropy, as well as to nearly-zero magnetostriction value of the material obtained by nanocrystallization of their amorphous precursors, and consisting of nano-sized grains, with average size about 10 nm, embedded in an amorphous matrix [57].

As discussed elsewhere, after nanocrystallization the average magnetostriction constant takes nearly - zero values [57,106], thanks to the control of the crystalline volume fraction: the existence of two phases (amorphous and crystalline) provides a good balance of a negative magnetostriction of α-Fe-Si nanocrystallites of about ($\lambda_s^{FeSi} \approx$ -6 x 10^{-6}) [48] and a positive one for the amorphous matrix of about ($\lambda_s^{am} \approx$ 20 x 10^{-6}) [48] resulting finally in vanishing net magnetostriction values [105]:

$$\lambda_s^{eff} \approx V_{cr}\, \lambda_s^{FeSi} + (1 - V_{cr})\, \lambda_s^{am} \qquad (7)$$

being $\lambda_s{}^{eff}$ the saturation magnetostriction coefficient, and V_{cr} denotes the crystalline volume fraction.

This nanocrystallization of FeSiBNbCu alloys is usually observed after annealing in the range of 500-600°C for 1 hour (i.e., at temperatures between the first and second crystallization stages). One of the examples of the evolution of the hysteresis loops of Finemet-type microwires upon nanocrystallization is shown in Figure 23. As can observed from Figure 23, in the case of the $Fe_{70.8}Cu_1Nb_{3.1}Si_{14.5}B_{10.6}$ microwire, annealing at T_{ann} up to 550 °C allows considerable decrease of coercivity. For these annealing conditions the character of hysteresis loops does not change: all the hysteresis loops present rectangular shape. In some cases rectangular hysteresis loops are reported not only upon devitrification of Finemet-type, but even after second crystallization process when values up to 2400 A/m are observed [107]. One of the examples is shown in Figure 24a, where hysteresis loop of $Fe_{71,8}Cu_1Nb_{3,1}Si_{15}B_{9,1}$ microwire (ρ=0.282) annealed at T_{ann} =700 °C is shown. However, $Fe_{71,8}Cu_1Nb_{3,1}Si_{15}B_{9,1}$ microwire (ρ=0.467) present rather different step-wise hysteresis loops (see Figure 24b) that can be attributed to partially crystalline (bi-phase) structure. Such partially crystalline magnetic microwires, with step-wise hysteresis loops related to magnetic interaction between crystals or mixed amorphous-crystalline structure, can be interesting for applications in electronic surveillance systems [108].

The microwires obtained by devitrification exhibit higher saturation magnetization and at certain annealing conditions can present better magnetic softness and GMI response than as-prepared Fe-rich microwires and therefore they are useful for GMI sensors and metacomposites applications [47].

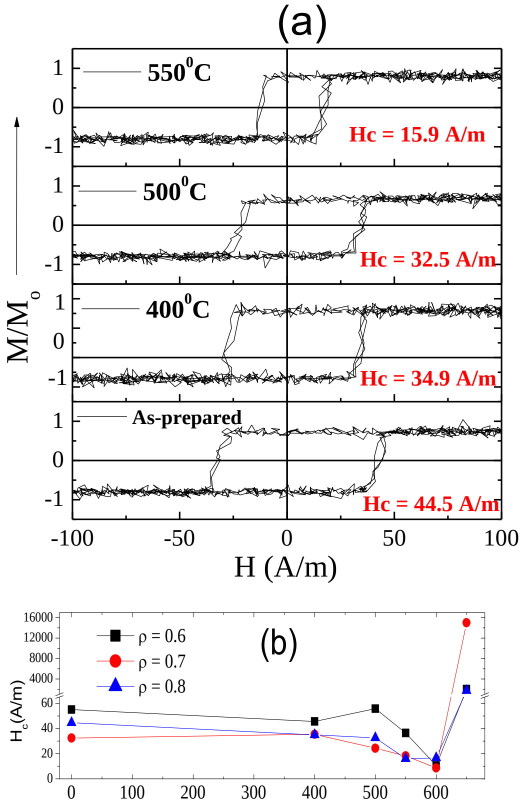

Figure 23 Hysteresis loops of as-prepared and annealed $Fe_{70.8}Cu_1Nb_{3.1}Si_{14.5}B_{10.6}$ microwire samples at T_{ann} between 400°C-600°C (a); coercive field dependence on T_{ann} of $Fe_{70.8}Cu_1Nb_{3.1}Si_{14.5}B_{10.6}$ for different ϱ-ratios (b). (Reproduced with permission from [48] Fig4 Copyright © 2016 Springer Nature)

In fact, microwires with nanocrystalline structure can be obtained even directly in as-prepared state without annealing [109, 110]. The advantage of such microwires is that they can present better mechanical properties [109,110].

It is worth mentioning, that the use of specially designed compositions allows further increase of saturation magnetization, $\mu_0 M_s$, [111] and also obtain extremely magnetically soft nanocrystalline materials. In the case of microwires, the use of a similar chemical composition allows preparation of nanocrystalline microwires with improved DW mobility without any post processing [109]. The partially crystalline $(Fe_{0.7}Co_{0.3})_{83.7}Si_4B_8P_{3.6}Cu_{0.7}$ microwire presents elevated values of H_c (about 480 A/m) and rather high saturation magnetization of about 1.6 T (see Figure 25).

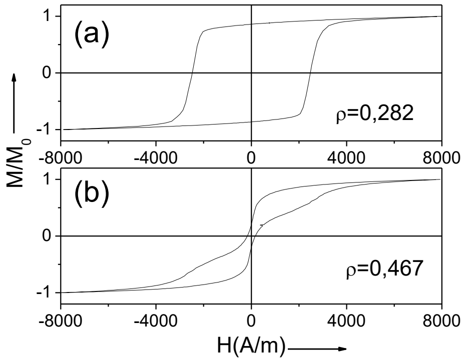

Figure 24. Hysteresis loops of $Fe_{71,8}Cu_1Nb_{3,1}Si_{15}B_{9,1}$ microwires with ρ=0,282 (a) and ρ =0,467 (b) annealed at 700°C. Adapted from ref. [107].

Such elevated H_c -values are quite similar to that exhibited by other partially nanocrystalline microwires, i.e., Hitperm-like $Fe_{38.5}Co_{38.5}B_{18}Mo_4Cu_1$ microwires with similar average grain size (about 38 nm and 23-33 nm for $(Fe_{0.7}Co_{0.3})_{83.7}Si_4B_8P_{3.6}Cu_{0.7}$ and Hitperm-like microwires, respectively) [110]. Accordingly, even partially crystalline or nanocrystalline microwires can present perfectly rectangular hysteresis loops. For $(Fe_{0.7}Co_{0.3})_{83.7}Si_4B_8P_{3.6}Cu_{0.7}$ microwire elevated $\mu_0 M_s$ -values allowed to obtain extremely fast domain wall velocity even in as-prepared state [110].

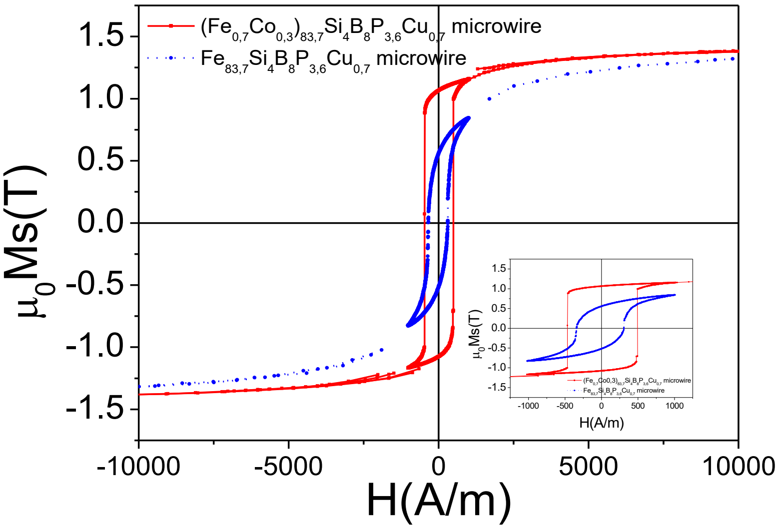

Figure 25. Hysteresis loops of studied $(Fe_{0.7}Co_{0.3})_{83.7}Si_4B_8P_{3.6}Cu_{0.7}$ and $Fe_{83.7}Si_4B_8P_{3.6}Cu_{0.7}$ (prepared for comparison) microwires as indicated. (Reproduced with permission from [109] Fig5 Copyright © 2020 Elsevier B.V)

Aforementioned Hitperm-like $Fe_{38.5}Co_{38.5}B_{18}Mo_4Cu_1$ microwires are the other example of nanocrystalline microwires with perfectly rectangular hysteresis loops (see Figure 26) and hence fast magnetization switching by single domain wall propagation [110]. Higher H_c -values of $Fe_{38.5}Co_{38.5}B_{18}Mo_4Cu_1$ and $(Fe_{0.7}Co_{0.3})_{83.7}Si_4B_8P_{3.6}Cu_{0.7}$ microwires have been attributed to elevated magnetostriction coefficient of these microwires as-compared to Finemet-type microwires.

On the other hand, magnetically hard and semi-hard wires are potentially quite interesting for various applications related to the design of smart markers for the electronic article surveillance, motors, compass needles and tachometers, magnetic microelectromechanical systems (magnetic MEMS), dentistry and for magnetic tips for magnetic force microscopy [112,113].

Recently a few successful attempts to achieve hard magnetic properties in microwires have been reported. Among others, various approaches are being developed to enhance hard magnetic behavior by employing novel alloys, i.e., Fe-Pt based alloys [114] or Heusler-type (Ni-Mn-Ga) alloys [115].

Peer-reviewed version available at Processes 2020, 8, 1006; doi:10.3390/pr8081006

Magnetic hardening in $Fe_{50}Pt_{40}Si_{10}$ microwires has been observed after annealing upon the formation of L10-type superstructure after crystallization of as-prepared amorphous precursor (see Figure 27). In this case after devitrification of amorphous $Fe_{50}Pt_{40}Si_{10}$ microwire H_c ≈40 kA/m is observed.

Magnetic hardening is also reported in Co-rich microwires annealed by Joule heating [116].

Consequently, magnetic properties of crystalline microwires depend on the chemical composition of the metallic nucleus and on structural features (grain size, precipitating phases) of either as-prepared or annealed microwire: crystalline microwire can exhibit either soft magnetic properties or semi-hard magnetic properties.

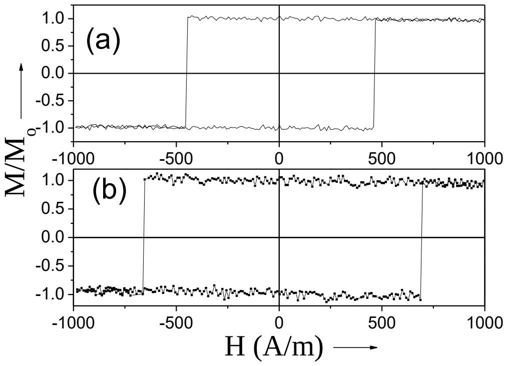

Figure 26. Hysteresis loops of as-prepared $Fe_{38.5}Co_{38.5}B_{18}Mo_4Cu_1$ microwires: sample 1 with ρ= 0.41 (a) and sample 2 with ρ= 0.6 (b) measured at f=50 Hz. (Reproduced with permission from [109] Fig1 Copyright © 2016 Elsevier B.V)

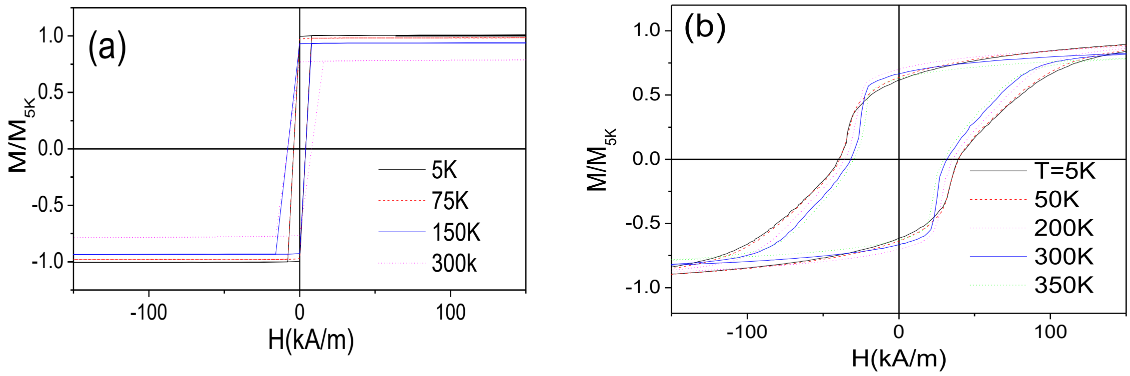

Figure 27. Hysteresis loops of as-prepared (a) and annealed at 500 °C for 1 h (b) $Fe_{50}Pt_{40}Si_{10}$ microwires measured at different temperatures. Adapted from ref. [114].

4. Conclusions

We showed that the magnetic properties of glass-coated microwires prepared by the Taylor-Ulitovsky method can be tuned in as-prepared state or further modified by appropriate post-processing.

Magnetic properties of amorphous magnetic microwires can be tuned either in as-prepared state or by controlling the magnetoelastic anisotropy through the magnetostriction coefficient value and by the internal stresses values related to the fabrication conditions and geometry of microwires. Furthermore, appropriate post-processing (including either conventional heat treatment, heat treatment in the presence of applied stress or magnetic field or glass-coating removal) allows further tuning of magnetic properties of magnetic microwires.

We showed that the microwires with coercivities from 1 A/m to 40 kA/m can be prepared.

Depending on the chemical composition of metallic nucleus as well as structural features (grain size, precipitating phases) prepared microwire can exhibit soft magnetic properties or semi-hard magnetic properties.

Author Contributions: Conceptualization, A.Z. and V.Z.; methodology, M.I., J.M.B. and V.Z.; validation, A.Z; formal analysis, A.Z.; investigation, A.Z., A.T., P.C.L, J.O., L.G.L. and V.Z.; resources, A.Z.; data curation, V.Z., P.C.L., J.M.B., M.I., L.G.L. and A.T.; writing—original draft preparation, A.Z.; writing—review and editing, A.Z., P.C.L., J.M.B., L.G.L. and A.T.; supervision, A.Z.; funding acquisition, A.Z. and V.Z. All authors have read and agreed to the published version of the manuscript.

Funding: This research was funded by Spanish MCIU under PGC2018-099530-B-C31 (MCIU/AEI/FEDER, UE), by the Government of the Basque Country under PIBA 2018-44 and Elkartek (CEMAP and AVANSITE) projects and by the University of Basque Country under the scheme of "Ayuda a Grupos Consolidados" (Ref.: GIU18/192).

Acknowledgments: Authors give thanks for technical and human support to SGIker of UPV/EHU (Medidas Magnéticas Gipuzcoa) and European funding (ERDF and ESF).

Conflicts of Interest: The authors declare no conflict of interest.

References

1. Lenz, J.; Edelstein, S. Magnetic sensors and their applications. *IEEE Sens. J.* **2006**, *6*, 631–649, doi:10.1109/JSEN.2006.874493.
2. Díaz-Michelena, M. Small Magnetic Sensors for Space Applications. *Sensors* **2009**, *9*, 2271–2288, doi:10.3390/s90402271.
3. Ripka, P.; Vértesy, G. Sensors based on soft magnetic materials Panel discussion. *J. Magn. Magn. Mater.* **2000**, *215–216*, 795–799, doi:10.1016/S0304-8853(00)00291-2.
4. Fiorillo, F.; Bertotti, G.; Appino, C.; Pasquale, M. Soft Magnetic Materials. In *Wiley Encyclopedia of Electrical and Electronics Engineering*; John Wiley & Sons, Inc, 2016; pp. 1–42 ISBN 978-0-471-34608-1.
5. Jiles, D.C. Recent advances and future directions in magnetic materials. *Acta Mater.* **2003**, *51*, 5907–5939, doi:10.1016/j.actamat.2003.08.011.
6. *High Performance Soft Magnetic Materials*; Zhukov, A., Ed.; Springer Series in Materials Science; Springer International Publishing, 2017; p. 216 ISBN 978-3-319-49705-1.
7. Mohri, K.; Humphrey, F.B.; Kawashima, K.; Kimura, K.; Mizutani, M. Large Barkhausen and Matteucci effects in FeCoSiB, FeCrSiB, and FeNiSiB amorphous wires. *IEEE Trans. Magn.* **1990**, *26*, 1789–1791, doi:10.1109/20.104526.
8. Ogasawara, I.; Ueno, S. Preparation and properties of amorphous wires. *IEEE Trans. Magn.* **1995**, *31*, 1219–1223, doi:10.1109/20.364811.
9. Vazquez, M.; Chen, D.-X. The magnetization reversal process in amorphous wires. *IEEE Trans. Magn.* **1995**, *31*, 1229–1238, doi:10.1109/20.364813.
10. Panina, L.V.; Mohri, K. Magneto-impedance effect in amorphous wires. *Appl. Phys. Lett.* **1994**, *65*, 1189–1191, doi:10.1063/1.112104.
11. Beach, R.S.; Berkowitz, A.E. Giant magnetic field dependent impedance of amorphous FeCoSiB wire. *Appl. Phys. Lett.* **1994**, *64*, 3652–3654, doi:10.1063/1.111170.
12. Zhukov, A.; Ipatov, M.; Zhukova, V. Chapter 2 - Advances in Giant Magnetoimpedance of Materials. In *Handbook of Magnetic Materials*; Buschow, K.H.J., Ed.; Elsevier, 2015; Vol. 24, pp. 139–236.
13. Knobel, M.; Vázquez, M.; Kraus, L. Giant Magnetoimpedance. In *Handbook of Magnetic Materials*; Handbook of Magnetic Materials; Elsevier, 2003; Vol. 15, pp. 497–563.
14. Harrison, E.P.; Turney, G.L.; Rowe, H. Electrical Properties of Wires of High Permeability. *Nature* **1935**, *135*, 961, doi:10.1038/135961a0.

Peer-reviewed version available at Processes 2020, 8, 1006; doi:10.3390/pr8081006

15. Sixtus, K.J.; Tonks, L. Propagation of Large Barkhausen Discontinuities. II. *Phys. Rev.* **1932**, *42*, 419–435, doi:10.1103/PhysRev.42.419.
16. Zhukov, A.P. The remagnetization process of bistable amorphous alloys. *Mater. Des.* **1993**, *14*, 299–306, doi:10.1016/0261-3069(93)90130-N.
17. Phan, M.-H.; Peng, H.-X.; Yu, S.-C.; Vázquez, M. Optimized giant magnetoimpedance effect in amorphous and nanocrystalline materials. *J. Appl. Phys.* **2006**, *99*, 08C505, doi:10.1063/1.2162089.
18. Zhukov, A.; Zhukova, V.; Blanco, J.M.; Gonzalez, J. Recent research on magnetic properties of glass-coated microwires. *J. Magn. Magn. Mater.* **2005**, *294*, 182–192, doi:10.1016/j.jmmm.2005.03.033.
19. Varga, R.; Richter, K.; Zhukov, A.; Larin, V. Domain Wall Propagation in Thin Magnetic Wires. *IEEE Trans. Magn.* **2008**, *44*, 3925–3930, doi:10.1109/TMAG.2008.2001997.
20. Corodeanu, S.; Chiriac, H.; Óvári, T.-A. Accurate measurement of domain wall velocity in amorphous microwires, submicron wires, and nanowires. *Rev. Sci. Instrum.* **2011**, *82*, 094701, doi:10.1063/1.3635223.
21. Biziere, N.; Gatel, C.; Lassalle-Balier, R.; Clochard, M.C.; Wegrowe, J.E.; Snoeck, E. Imaging the Fine Structure of a Magnetic Domain Wall in a Ni Nanocylinder. *Nano Lett.* **2013**, *13*, 2053–2057, doi:10.1021/nl400317j.
22. Da Col, S.; Jamet, S.; Staňo, M.; Trapp, B.; Le Denmat, S.; Cagnon, L.; Toussaint, J.C.; Fruchart, O. Nucleation, imaging, and motion of magnetic domain walls in cylindrical nanowires. *Appl. Phys. Lett.* **2016**, *109*, 062406, doi:10.1063/1.4961058.
23. Blanco, J.M.; Zhukova, V.; Ipatov, M.; Zhukov, A. Magnetic Properties and Domain Wall Propagation in Micrometric Amorphous Microwires. *Sens. Lett.* **2013**, *11*, 187-190(4), doi:info:doi/10.1166/sl.2013.2782.
24. Óvári, T.-A.; Corodeanu, S.; Chiriac, H. Domain wall velocity in submicron amorphous wires. *J. Appl. Phys.* **2011**, *109*, 07D502, doi:10.1063/1.3536797.
25. Pirota, K.R.; Kraus, L.; Chiriac, H.; Knobel, M. Magnetic properties and giant magnetoimpedance in a CoFeSiB glass-covered microwire. *J. Magn. Magn. Mater.* **2000**, *221*, L243–L247, doi:10.1016/S0304-8853(00)00554-0.
26. Corte-León, P.; Zhukova, V.; Ipatov, M.; Blanco, J.M.; Gonzalez, J.; Zhukov, A. Engineering of magnetic properties of Co-rich microwires by joule heating. *Intermetallics* **2019**, *105*, 92–98, doi:10.1016/j.intermet.2018.11.013.
27. Mohri, K.; Uchiyama, T.; Panina, L.V.; Yamamoto, M.; Bushida, K. Recent Advances of Amorphous Wire CMOS IC Magneto-Impedance Sensors: Innovative High-Performance Micromagnetic Sensor Chip Available online: https://www.hindawi.com/journals/js/2015/718069/abs/ (accessed on Jan 18, 2019).
28. Honkura, Y.; Honkura, S. The Development of ASIC Type GSR Sensor Driven by GHz Pulse Current. *Sensors* **2020**, *20*, 1023, doi:10.3390/s20041023.
29. Sandacci, S.; Makhnovskiy, D.; Panina, L.; Mohri, K.; Honkura, Y. Off-diagonal impedance in amorphous wires and its application to linear magnetic sensors. *IEEE Trans. Magn.* **2004**, *40*, 3505–3511, doi:10.1109/TMAG.2004.835676.
30. Dufay, B.; Saez, S.; Dolabdjian, C.; Yelon, A.; Menard, D. Development of a High Sensitivity Giant Magneto-Impedance Magnetometer: Comparison With a Commercial Flux-Gate. *IEEE Trans. Magn.* **2013**, *49*, 85–88, doi:10.1109/TMAG.2012.2219579.
31. Uchiyama, T.; Mohri, K.; Nakayama, S. Measurement of Spontaneous Oscillatory Magnetic Field of Guinea-Pig Smooth Muscle Preparation Using Pico-Tesla Resolution Amorphous Wire Magneto-Impedance Sensor. *IEEE Trans. Magn.* **2011**, *47*, 3070–3073, doi:10.1109/TMAG.2011.2148165.

Peer-reviewed version available at *Processes* **2020**, *8*, 1006; doi:10.3390/pr8081006

32. Cobeño, A.F.; Zhukov, A.; Blanco, J.M.; Larin, V.; Gonzalez, J. Magnetoelastic sensor based on GMI of amorphous microwire. *Sens. Actuators Phys.* **2001**, *91*, 95–98, doi:10.1016/S0924-4247(01)00502-7.
33. Zhukova, V.; Blanco, J.M.; Ipatov, M.; Zhukov, A.; García, C.; Gonzalez, J.; Varga, R.; Torcunov, A. Development of thin microwires with low Curie temperature for temperature sensors applications. *Sens. Actuators B Chem.* **2007**, *126*, 318–323, doi:10.1016/j.snb.2007.02.019.
34. Ulitovsky, A. V., Maianski, I. M., Avramenco, A. I., "Method of continuous casting of glass coated microwire", USSR Patent, No. 128427, 15.05.60. Bulletin No. 10, p. 14.
35. Kraus, L., Schneider, J. and Wiesner, H., Ferromagnetic resonance in amorphous alloys prepared by rapid quenching from the melt, *Czech. J. Phys. B*, **1976**, 26, 601-602.
36. Zhukov, A.; Ipatov, M.; Talaat, A.; Blanco, J.M.; Hernando, B.; Gonzalez-Legarreta, L.; Suñol, J.J.; Zhukova, V. Correlation of Crystalline Structure with Magnetic and Transport Properties of Glass-Coated Microwires. *Crystals* **2017**, *7*, 41, doi:10.3390/cryst7020041.
37. Baranov, S.A.; Larin, V.S.; Torcunov, A.V. Technology, Preparation and Properties of the Cast Glass-Coated Magnetic Microwires. *Crystals* **2017**, *7*, 136, doi:10.3390/cryst7060136.
38. Zhukova, V.; Blanco, J. M.; Ipatov, M.; Zhukov, A. Magnetoelastic Contribution in Domain-Wall Dynamics of Magnetically Bistable Microwires, IEEE Trans. Magn. , **2011**, *47(10)*, 3783-3787, doi: 10.1109/TMAG.2011.2158193.
39. Zhukov, A.; Gonzalez, J.; Zhukova, V. Magnetoresistance in thin wires with granular structure. *J. Magn. Magn. Mater.* **2005**, *294*, 165–173, doi:10.1016/j.jmmm.2005.03.031.
40. Zhukov, A.; Rodionova, V.; Ilyn, M.; Aliev, A.M.; Varga, R.; Michalik, S.; Aronin, A.; Abrosimova, G.; Kiselev, A.; Ipatov, M.; et al. Magnetic properties and magnetocaloric effect in Heusler-type glass-coated NiMnGa microwires. *J. Alloys Compd.* **2013**, *575*, 73–79, doi:10.1016/j.jallcom.2013.04.083.
41. Zhukova, V.; Talaat, A.; del Val, J.J.; Ipatov, M.; Zhukov, A. Preparation and Characterization of Fe-Pt and Fe-Pt-(B, Si) Microwires, *IEEE Magn. Lett.*, **2016**, *7*, 5200704, doi: 10.1109/LMAG.2015.2506549
42. Zhukova, V.; Corte-Leon, P.; Ipatov, M.; Blanco, J.M.; Gonzalez-Legarreta, L.; Zhukov, A. Development of Magnetic Microwires for Magnetic Sensor Applications. *Sensors* **2019**, *19*, 4767, doi:10.3390/s19214767.
43. Zhukov, A.; Ipatov, M.; Corte-León, P.; Gonzalez-Legarreta, L.; Blanco, J.M.; Zhukova, V. Soft magnetic microwires for sensor applications. *J. Magn. Magn. Mater.* **2020**, *498*, 166180, doi:10.1016/j.jmmm.2019.166180.
44. Antonov, A.S.; Borisov, V.T.; Borisov, O.V.; Prokoshin, A.F.; Usov, N.A. Residual quenching stresses in glass-coated amorphous ferromagnetic microwires. *J. Phys. Appl. Phys.* **2000**, *33*, 1161, doi:10.1088/0022-3727/33/10/305.
45. Zhukova, V.; Blanco, J.M.; Ipatov, M.; Zhukov, A. Magnetoelastic contribution in domain wall dynamics of amorphous microwires, *Physica B* **2012**, *407*, 1450–1454, doi:10.1016/j.physb.2011.09.124
46. Zhukov, A.; Cobeño, A.F.; Gonzalez, J.; Torcunov, A.; Pina, E.; Prieto, M.J.; Blanco, J.M.; Larin, V.; Baranov, S. Ferromagnetic resonance, magnetic behaviour and structure of Fe-based glass-coated microwires. *J. Magn. Magn. Mater.* **1999**, *203*, 238–240, doi:10.1016/S0304-8853(99)00240-1.
47. Velázquez, J.; Vázquez, M.; Hernando, A.; Savage, H.T.; Wun-Fogle, M. Magnetoelastic anisotropy in amorphous wires due to quenching. *J. Appl. Phys.* **1991**, *70*, 6525–6527, doi:10.1063/1.349895.
48. Talaat, A.; Zhukova, V.; Ipatov, M.; del Val, J.J.; Blanco, J.M.; Gonzalez-Legarreta, L.; Hernando, B.; Churyukanova, M.; Zhukov, A. Engineering of Magnetic Softness and Magnetoimpedance in Fe-Rich Microwires by Nanocrystallization. *JOM* **2016**, *68*, 1563–1571, doi:10.1007/s11837-016-1889-y.

49. Gonzalez-Legarreta, L.; Corte-León, P.; Zhukova, V.; Ipatov, M.; Blanco, J.M.; Churyukanova, M.; Taskaev, S.; Zhukov, A. Route of magnetoimpedance and domain walls dynamics optimization in Co-based microwires. *J. Alloys Compd.* **2020**, *830*, 154576, doi:10.1016/j.jallcom.2020.154576.
50. Goto, T.; Nagano, M.; Wehara, N. Mechanical Properties of Amorphous Fe80P16C3B1 Filament Produced by Glass-Coated Melt Spinning. *Trans. Jpn. Inst. Met.* **1977**, *18*, 759–764, doi:10.2320/matertrans1960.18.759.
51. Zhukova, V.; Cobeño, A.F.; Zhukov, A.; de Arellano Lopez, A.R.; Blanco, J.M.; Larin, V.; Gonzalez, J.; López-Pombero, S. Correlation between magnetic and mechanical properties of devitrified glass-coated Fe71.8Cu1Nb3.1Si15B9.1 microwires. *J. Magn. Magn. Mater.* **2002**, *249*, 79–84, doi:10.1016/S0304-8853(02)00509-7.
52. Corte-León, P.; Gonzalez-Legarreta, L.; Zhukova, V.; Ipatov, M.; Blanco, J.M.; Churyukanova, M.; Taskaev, S.; Zhukov, A. Controlling the domain wall dynamics in Fe-, Ni- and Co-based magnetic microwires. *J. Alloys Compd.* **2020**, *834*, 155170, doi:10.1016/j.jallcom.2020.155170.
53. Zhukov, A.; Talaat, A.; Ipatov, M.; Zhukova, V. Tailoring the High-Frequency Giant Magnetoimpedance Effect of Amorphous Co-Rich Microwires. *IEEE Magn. Lett.* **2015**, *6*, 1–4, doi:10.1109/LMAG.2015.2397877.
54. Zhukov, A.; Churyukanova, M.; Kaloshkin, S.; Sudarchikova, V.; Gudoshnikov, S.; Ipatov, M.; Talaat, A.; Blanco, J.M.; Zhukova, V. Magnetostriction of Co–Fe-Based Amorphous Soft Magnetic Microwires. *J. Electron. Mater.* **2016**, *45*, 226–234, doi:10.1007/s11664-015-4011-2.
55. Churyukanova, M.; Semenkova, V.; Kaloshkin, S.; Shuvaeva, E.; Gudoshnikov, S.; Zhukova, V.; Shchetinin, I.; Zhukov, A. Magnetostriction investigation of soft magnetic microwires. *Phys. Status Solidi A* **2016**, *213*, 363–367, doi:10.1002/pssa.201532552.
56. Konno, Y.; Mohri, K. Magnetostriction measurements for amorphous wires. *IEEE Trans. Magn.* **1989**, *25*, 3623–3625, doi:10.1109/20.42381.
57. Herzer, G. Amorphous and nanocrystalline soft magnets. In Proceedings of the NATO Advanced Study Insititute on Magnetic Hysteresis in Novel Materials, Mykonos, Greece, 1–12 July 1996; Hadjipanayis, G.C., Ed.; NATO ASI Series (Series E: Applied Sciences), Kluwer Academic Publishers: Dordrecht, The Netherlands, 1997; Volume 338, pp. 711–730.
58. Cobeño, A. F.; Zhukov, A.; Blanco J. M.; Gonzalez, J. Giant magneto-impedance effect in CoMnSiB amorphous microwires, *J. Magn. Magn. Mater.* **2001**, *234*, L359-L365
59. Corte-Leon, P.; Zhukova, V.; Blanco, J. M.; González- Legarreta, L.; Ipatov M. and A. Zhukov,A., Stress-induced Magnetic Anisotropy Enabling Engineering of Magnetic Softness of Fe-rich Amorphous Microwires, *J. Magn. Magn. Mater.* **2020**, *510*,166939, doi: https://doi.org/10.1016/j.jmmm.2020.166939
60. Zhukova, V.; Blanco, J.M.; Chizhik, A.; Ipatov, M.; Zhukov, A. AC-current-induced magnetization switching in amorphous microwires. *Front. Phys.* **2018**, *13*, 137501, doi:10.1007/s11467-017-0722-6.
61. Zhukova, V.; Zhukov, A.; Blanco, J.M.; Gonzalez, J.; Ponomarev, B.K. Switching field fluctuations in a glass-coated Fe-rich amorphous microwire. *J. Magn. Magn. Mater.* **2002**, *249*, 131–135, doi:10.1016/S0304-8853(02)00520-6.
62. Chiriac, H.; Óvári, T.-A.; Corodeanu, S.; Ababei, G. Interdomain wall in amorphous glass-coated microwires. *Phys. Rev. B* **2007**, *76*, 214433, doi:10.1103/PhysRevB.76.214433.
63. Astefanoaei, I.; Radu, D.; Chiriac, H. Internal stress distribution in DC joule-heated amorphous glass-covered microwires. *J. Phys. Condens. Matter* **2006**, *18*, 2689–2716, doi:10.1088/0953-8984/18/9/008.
64. Chiriac, H.; Óvári, T.A.; Pop, Gh. Internal stress distribution in glass-covered amorphous magnetic wires. *Phys. Rev. B* **1995**, *52*, 10104–10113, doi:10.1103/PhysRevB.52.10104.

65. García-Prieto, M.J.; Pina, E.; Zhukov, A.; Larin, V.; Marín, P.; Vázquez, M.; Hernando, A. Glass-coated Co-rich amorphous microwires with enhanced permeability. *Sens. Actuators A Phys.* **2000**, *81*, 227–231, doi:10.1016/S0924-4247(99)00129-6.
66. Catalan, C.F.; Prida, V.M; Alonso, J; Vázquez, M; Zhukov, A; Hernando, B; Velázquez, J;, Effect of glass coating on magnetic properties of amorphous microwires, Rapidly Quenched & Metastable Materials, *Materials Science & Engineering A, Supplement*, **1997**, 438-441.
67. Takajo, M.; Yamasaki, J.; Humphrey, F.B. Domain structure of chemically thinned Fe-Si-B amorphous wires. *IEEE Trans. Magn.* **1999**, *35*, 3904–3906, doi:10.1109/20.800703.
68. Kabanov, Yu.; Zhukov, A.; Zhukova, V.; Gonzalez, J. Magnetic domain structure of wires studied by using the magneto-optical indicator film method. *Appl. Phys. Lett.* **2005**, *87*, 142507, doi:10.1063/1.2077854.
69. Usov, N.; Antonov, A.; Dykhne, A.; Lagar'kov, A. Possible origin for the bamboo domain structure in Co-rich amorphous wire. *J. Magn. Magn. Mater.* **1997**, *174*, 127–132, doi:10.1016/S0304-8853(97)00130-3.
70. Nderu, J.N.; Takajo, M.; Yamasaki, J.; Humphrey, F.B. Effect of stress on the bamboo domains and magnetization process of CoSiB amorphous wire. *IEEE Trans. Magn.* **1998**, *34*, 1312–1314, doi:10.1109/20.706532.
71. Corte-Leon, P.; Zhukova, V.; Ipatov, M.; Blanco, J.M.; Gonzalez, J.; Churyukanova, M.; Baraibar, J.M.; Taskaev, S.; Zhukov, A. Stress dependence of the magnetic properties of glass-coated amorphous microwires. *J. Alloys Compd.* **2019**, *789*, 201–208, doi:10.1016/j.jallcom.2019.03.044.
72. Barandiarán, J.M.; Hernando, A.; Madurga, V.; Nielsen, O.V.; Vázquez, M.; Vázquez-López, M. Temperature, stress, and structural-relaxation dependence of the magnetostriction in $(Co_{0.94}Fe_{0.06})_{75}Si_{15}B_{10}$ glasses. *Phys. Rev. B* **1987**, *35*, 5066–5071, doi:10.1103/PhysRevB.35.5066.
73. Zhukov, A.; Ipatov, M.; Gonzalez, J.; Blanco, J.M.; Zhukova, V. Recent advances in studies of magnetically soft amorphous microwires. *J. Magn. Magn. Mater.* **2009**, *321*, 822–825, doi:10.1016/j.jmmm.2008.11.068.
74. Zhukov, A.; Ipatov, M.; Corte-León, P.; Legarreta, L.G.-; Churyukanova, M.; Blanco, J.M.; Gonzalez, J.; Taskaev, S.; Hernando, B.; Zhukova, V. Giant magnetoimpedance in rapidly quenched materials. *J. Alloys Compd.* **2020**, *814*, 152225, doi:10.1016/j.jallcom.2019.152225.
75. Zhukov, A.; González, J.; Blanco, J.M.; Vázquez, M.; Larin, V. Microwires coated by glass: A new family of soft and hard magnetic materials. *J. Mater. Res.* **2000**, *15*, 2107–2113, doi:10.1557/JMR.2000.0303.
76. Allwood, D.A.; Xiong, G.; Faulkner, C.C.; Atkinson, D.; Petit, D.; Cowburn, R.P. Magnetic Domain-Wall Logic. *Science* **2005**, *309*, 1688–1692, doi:10.1126/science.1108813.
77. Moriya, R.; Hayashi, M.; Thomas, L.; Rettner, C.; Parkin, S.S.P. Dependence of field driven domain wall velocity on cross-sectional area in Ni65Fe20Co15 nanowires. *Appl. Phys. Lett.* **2010**, *97*, 142506, doi:10.1063/1.3494521.
78. Zhukova, V.; Blanco, J.M.; Rodionova, V.; Ipatov, M.; Zhukov, A. Domain wall propagation in micrometric wires: Limits of single domain wall regime. *J. Appl. Phys.* **2012**, *111*, 07E311, doi:10.1063/1.3672076.
79. Zhukova, V.; Blanco, J.M.; Rodionova, V.; Ipatov, M.; Zhukov, A. Fast magnetization switching in Fe-rich amorphous microwires: Effect of magnetoelastic anisotropy and role of defects. *J. Alloys Compd.* **2014**, *586*, S287–S290, doi:10.1016/j.jallcom.2012.09.039.
80. Aragoneses, P.; Blanco, J.M.; Dominguez, L.; González, J.; Zhukov A.; Vázquez, M. The Stress dependence of the switching field in glass-coated amorphous microwires, *J. Phys. D: Applied Phys.* **1998**, *31*, 3040-3045, doi: 10.1088/0022-3727/31/21/009

81. Zhukova, V.; Talaat, A.; Corte-Leon, P.; Blanco, J.M.; Ipatov, M.; Zhukov, A. Engineering of magnetic properties and domain wall dynamics in Fe-Ni-based amorphous microwires by annealing. *AIP Adv.* **2020**, *10*, 015130, doi:10.1063/1.5130173..
82. Zhukov, A.; Churyukanova, M.; Kaloshkin, S.; Semenkova, V.; Gudoshnikov, S.; Ipatov, M.; Talaat, A.; Blanco, J.M.; Zhukova, V. Effect of annealing on magnetic properties and magnetostriction coefficient of Fe–Ni-based amorphous microwires. *J. Alloys Compd.* **2015**, *651*, 718–723, doi:10.1016/j.jallcom.2015.08.151.
83. Luborsky, F.; Walter, J. Magnetic anneal anisotropy in amorphous alloys. *IEEE Trans. Magn.* **1977**, *13*, 953–956, doi:10.1109/TMAG.1977.1059494.
84. Haimovich, J.; Jagielinski, T.; Egami, T. Magnetic and structural effects of anelastic deformation of an amorphous alloy. *J. Appl. Phys.* **1985**, *57*, 3581–3583, doi:10.1063/1.335013.
85. Zhukova, V.; Korchuganova, O.A.; Aleev, A.A.; Tcherdyntsev, V.V.; Churyukanova, M.; Medvedeva, E.V.; Seils, S.; Wagner, J.; Ipatov, M.; Blanco, J.M.; et al. Effect of annealing on magnetic properties and structure of Fe-Ni based magnetic microwires. *J. Magn. Magn. Mater.* **2017**, *433*, 278–284, doi:10.1016/j.jmmm.2017.03.028.
86. Zhukova, V.; Blanco, J.M.; Ipatov, M.; Gonzalez, J.; Churyukanova, M.; Zhukov, A. Engineering of magnetic softness and giant magnetoimpedance effect in Fe-rich microwires by stress-annealing. *Scr. Mater.* **2018**, *142*, 10–14, doi:10.1016/j.scriptamat.2017.08.014.
87. Zhukova, V.; Blanco, J.M.; Ipatov, M.; Churyukanova, M.; Taskaev, S.; Zhukov, A. Tailoring of magnetoimpedance effect and magnetic softness of Fe-rich glass-coated microwires by stress- annealing. *Sci. Rep.* **2018**, *8*, 1–14, doi:10.1038/s41598-018-21356-3.
88. Yamasaki, J.; Mohri, K.; Watari, K.; Narita, K. Domain wall induced anisotropy during annealing in amorphous ribbons. *IEEE Trans. Magn.* **1984**, *20*, 1855–1857, doi:10.1109/TMAG.1984.1063345.
89. Kohmoto, O.; Ohya, K. Amorphous FeCo-SiB alloys with zero magnetostriction. *J. Appl. Phys.* **1981**, *52*, 928–932, doi:10.1063/1.328778.
90. Becker, J.; Luborsky, F.; Walter, J. Magnetic moments and curie temperatures of (Fe, Ni)80(P, B)20amorphous alloys. *IEEE Trans. Magn.* **1977**, *13*, 988–991, doi:10.1109/TMAG.1977.1059499.
91. Rancourt, D.G.; Dang, M.-Z. Relation between anomalous magnetovolume behavior and magnetic frustration in Invar alloys. *Phys. Rev. B* **1996**, *54*, 12225–12231, doi:10.1103/PhysRevB.54.12225.
92. Gaskell, P.H. On the structure of simple inorganic amorphous solids. *J. Phys. C Solid State Phys.* **1979**, *12*, 4337–4368, doi:10.1088/0022-3719/12/21/004.
93. Zhukov, A.; Chichay, K.; Talaat, A.; Rodionova, V.; Blanco, J.M.; Ipatov, M.; Zhukova, V. Manipulation of magnetic properties of glass-coated microwires by annealing. *J. Magn. Magn. Mater.* **2015**, *383*, 232–236, doi:10.1016/j.jmmm.2014.10.003.
94. Zhukov, A.; Talaat, A.; Churyukanova, M.; Kaloshkin, S.; Semenkova, V.; Ipatov, M.; Blanco, J.M.; Zhukova, V. Engineering of magnetic properties and GMI effect in Co-rich amorphous microwires. *J. Alloys Compd.* **2016**, *664*, 235–241, doi:10.1016/j.jallcom.2015.12.224.
95. Corte-León, P.; Talaat, A.; Zhukova, V.; Ipatov, M.; Blanco, J.M.; Gonzalez, J.; Zhukov, A. Stress-Induced Magnetic Anisotropy Enabling Engineering of Magnetic Softness and GMI Effect of Amorphous Microwires. *Appl. Sci.* **2020**, *10*, 981, doi:10.3390/app10030981.
96. Zhukov, A.; Talaat, A.; Blanco, J.M.; Ipatov, M.; Zhukova, V. Tuning of Magnetic Properties and GMI Effect of Co-Based Amorphous Microwires by Annealing. *J. Electron. Mater.* **2014**, *43*, 4532–4539, doi:10.1007/s11664-014-3348-2.

97. Aragoneses, P.; Blanco J. M.; Cobeño, A.F.; L. Dominguez,L.; Gonzalez, J.; Zhukov A.; Larin, V. Stress Dependence of the Switching Field in Co-rich Amorphous Microwires, *J. Magn. Magn Mater.* **1999**, *196-197*, 248-250.

98. Corte-León, P.; Blanco, J.M.; Zhukova, V.; Ipatov, M.; Gonzalez, J.; Churyukanova, M.; Taskaev, S.; Zhukov, A. Engineering of Magnetic Softness and Domain Wall Dynamics of Fe-rich Amorphous Microwires by Stress- induced Magnetic Anisotropy. *Sci. Rep.* **2019**, *9*, 12427, doi:10.1038/s41598-019-48755-4.

99. Larin, V.S.; Zhukova, V.; Zhukov, A.; Torcunov, A.V.; Vazquez, M. Tailoring of magnetic anisotropy in Fe-rich glass-coated magnetic microwires by thermo-mechanical annealing. *Sens. Actuators A Phys.* **2003**, *106*, 96–100, doi:10.1016/S0924-4247(03)00142-0.

100. Zhukov, A.; Zhukova, V.; Larin, V.; Gonzalez, J. Tailoring of magnetic anisotropy of Fe-rich microwires by stress induced anisotropy. *Phys. B Condens. Matter* **2006**, *384*, 1–4, doi:10.1016/j.physb.2006.05.018.

101. Gonzalez-Legarreta, L.; Corte-Leon, P.; Zhukova, V.; Ipatov, M.; Blanco, J.M.; Gonzalez, J.; Zhukov, A. Optimization of magnetic properties and GMI effect of Thin Co-rich Microwires for GMI Microsensors. *Sensors* **2020**, *20*, 1558, doi:10.3390/s20061558.

102. Chichay, K; Rodionova, V; Ipatov, M; Zhukova, V; Zhukov, A. Effect of Temperature and Time of Stress Annealing on Magnetic Properties of Amorphous Microwires. *Acta Phys. Polonica* A **2015**, 127 600-602

103. Corte-León, P.; Zhukova, V.; Ipatov, M.; Blanco, J.M.; González, J.; Zhukov, A. Optimization of GMI Effect and Magnetic Properties of Co-Rich Microwires by Joule Heating. *IEEE Trans. Magn.* **2019**, *55*, 1–4, doi:10.1109/TMAG.2018.2868895.

104. Zhukova, V.; Cobeño, A.F.; Zhukov, A.; Blanco, J.M.; Puerta, S.; Gonzalez, J.; Vázquez, M. Tailoring of magnetic properties of glass-coated microwires by current annealing. *J. Non-Cryst. Solids* **2001**, *287*, 31–36, doi:10.1016/S0022-3093(01)00536-1.

105. Becker, J. A new mechanism for magnetic annealing in amorphous metals. *IEEE Trans. Magn.* **1978**, *14*, 938–940, doi:10.1109/TMAG.1978.1059842.

106. Zhukov, A.P.; Talaat, A.; Ipatov, M.; Blanco, J.M.; Gonzalez-Legarreta, L.; Hernando, B.; Zhukova, V. Effect of Nanocrystallization on Magnetic Properties and GMI Effect of Microwires. *IEEE Trans. Magn.* **2014**, *50*, 1–5, doi:10.1109/TMAG.2014.2303396.

107. Zhukova, V.; Cobeño, A.F.; Zhukov, A.; Blanco, J.M.; Larin, V.; Gonzalez, J. Coercivity of glass-coated Fe73.4-xCu1Nb3.1Si13.4+xB9.1 (0≤x≤1.6) microwires. *Nanostruct. Mater.* **1999**, *11*, 1319–1327, doi:10.1016/S0965-9773(99)00424-9.

108. Rodionova, V.; Ipatov, M.; Ilyn, M.; Zhukova, V.; Perov, N.; Gonzalez, J.; Zhukov, A. Tailoring of Magnetic Properties of Magnetostatically-Coupled Glass-Covered Magnetic Microwires. *J. Supercond. Nov. Magn.* **2011**, *24*, 541–547, doi:10.1007/s10948-010-0989-0.

109. Zhukova, V.; Ipatov, M.; Corte-Leon, P.; Blanco, J.M.; Zanaeva, E.; Bazlov, A.I.; Jiang, J.; Louzguine-Luzgin, D.V.; Olivera, J.; Zhukov, A. Excellent magnetic properties of (Fe0.7Co0.3)83.7Si4B8P3.6Cu0.7 ribbons and microwires. *Intermetallics* **2020**, *117*, 106660, doi:10.1016/j.intermet.2019.106660.

110. Talaat, A.; Del Val, J.J.; Zhukova, V.; Ipatov, M.; Klein, P.; Varga, R.; Gonzalez, J.; Zhdanova, M.; Churyukanova, M.; Zhukov, A. Effect of annealing on magnetic properties of nanocrystalline Hitperm-type glass-coated microwires. *J. Alloys Compd.* **2016**, *660*, 297–303, doi:10.1016/j.jallcom.2015.11.102.

111. Zhang, Y.; Sharma, P.; Makino, A. Effects of minor precipitation of large size crystals on magnetic properties of Fe-Co-Si-B-P-Cu alloy. *J. Alloys Compd.* **2017**, *709*, 663–667, doi:10.1016/j.jallcom.2017.03.193.

Peer-reviewed version available at *Processes* **2020**, *8*, 1006; doi:10.3390/pr8081006

112. Cordery, R.A.; III, C.F.M. Deactivatable electronic article surveillance markers using short semi-hard magnetic wires. US Patrent (1993) 5191315
113. Ferri, A.F.A; Pereira-da-Silva, M.A; Marega E. Jr. Magnetic Force Microscopy: Basic Principles and Applications, Atomic Force Microscopy - Imaging, Measuring and Manipulating Surfaces at the Atomic Scale, Dr. Victor Bellitto (Ed.), InTech, (2012) ISBN: 978-953-51-0414-8
114. Zhukov, A.; Ipatov, M.; Talaat, A.; Aronin, A.; Abrosimova, G.; del Val, J.J.; Zhukova, V. Magnetic hardening of Fe-Pt and Fe-Pt- M (M=B, Si) microwires. *J. Alloys Compd.* **2018**, *735*, 1071–1078, doi:10.1016/j.jallcom.2017.11.187
115. Zhukov, A.; Ipatov, M.; del Val, J.J.; Churyukanova, M.; Zhukova, V. Tailoring of magnetic properties of Heusler-type glass-coated microwires by annealing. *J. Alloys Compd.* **2018**, *732*, 561–566, doi:10.1016/j.jallcom.2017.10.232.
116. Evstigneeva, S.A.; Nematov, M.G.; Omelyanchik, A.; Yudanov, N.A.; Rodionova, V.V.; Panina, L.V. Hard Magnetic Properties of Co-Rich Microwires Crystallized by Current Annealing. *IEEE Magn. Lett.* **2020**, *11*, 1–5, doi:10.1109/LMAG.2020.2974152.